



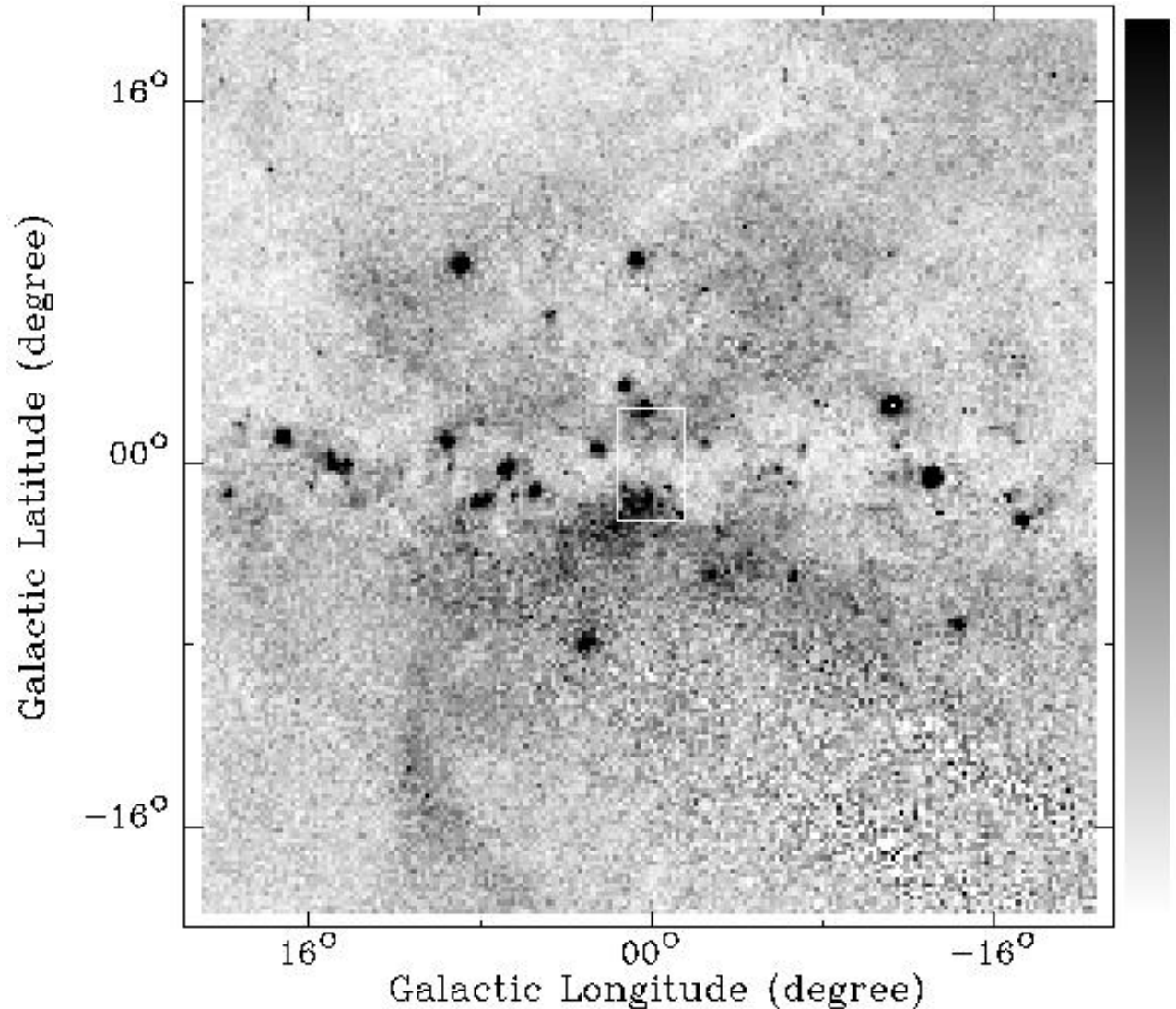
New insights on Starburst vs AGN driven winds

J. Bland-Hawthorn (U Sydney)

The Galaxy's bipolar wind is seen on 10 kpc scales...

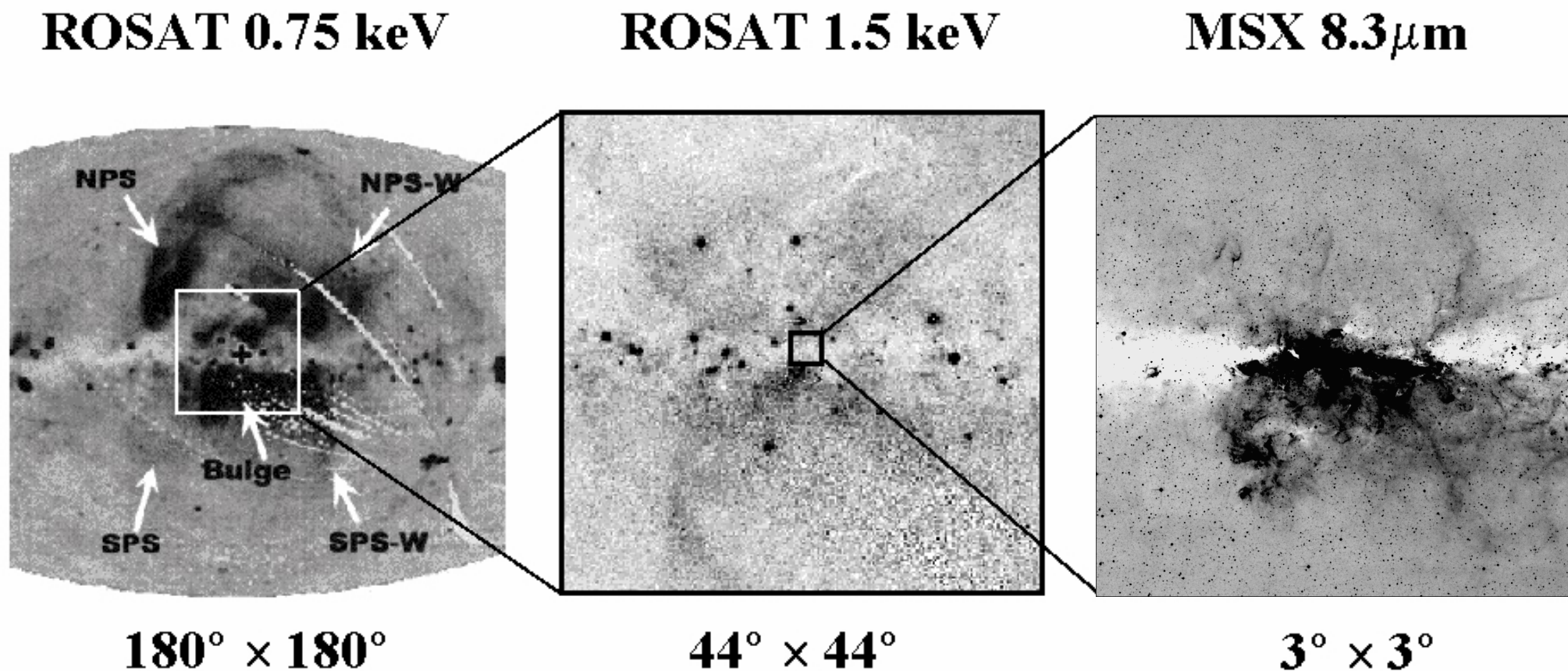
AGN or starburst driven?

ROSAT 1.5 keV (diffuse)

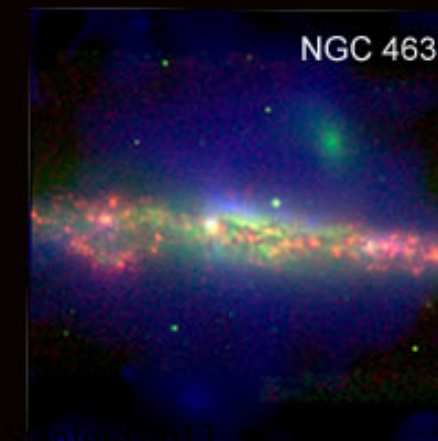
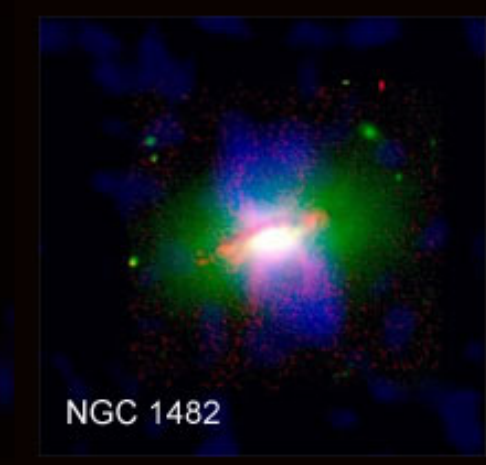
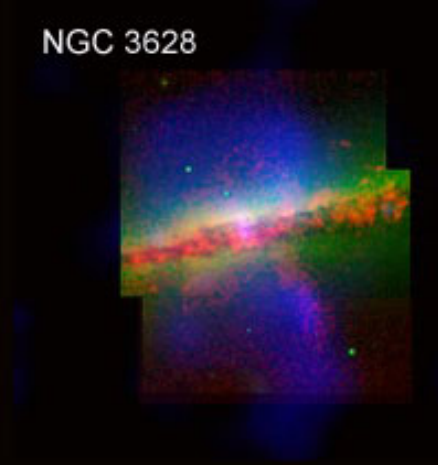
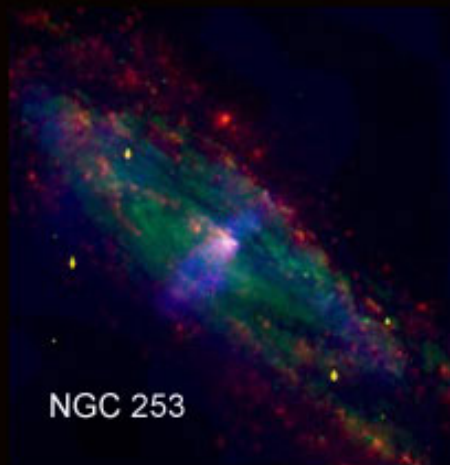
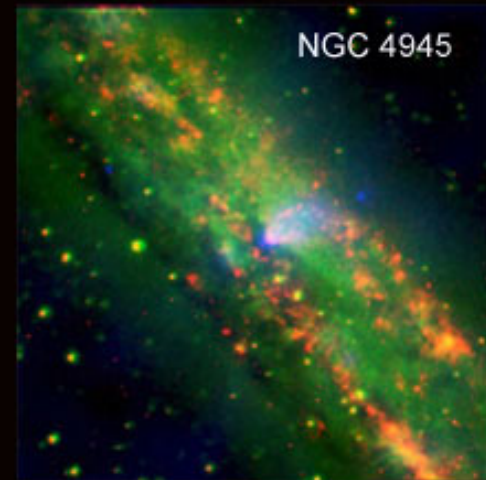
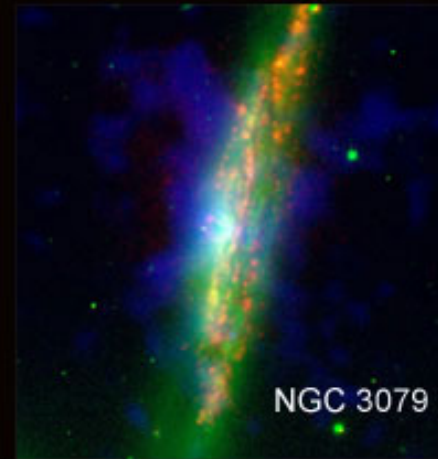
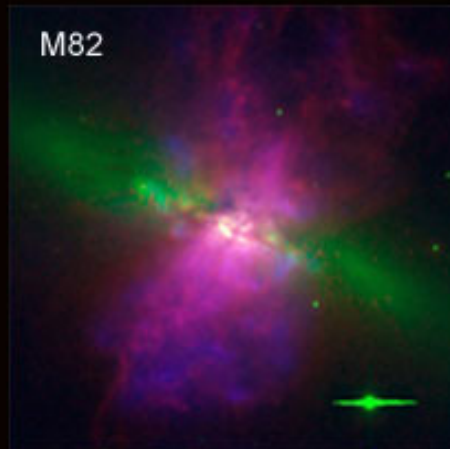


Two key observations: (1) bipolar structure not seen in soft X
(2) hard X bipolar structure never seen in OB blow-outs

JBH & Cohen (2003)



Very energetic winds may be common to all galaxies and be very difficult to detect...



Galactic winds arise in
both ★B and AGN

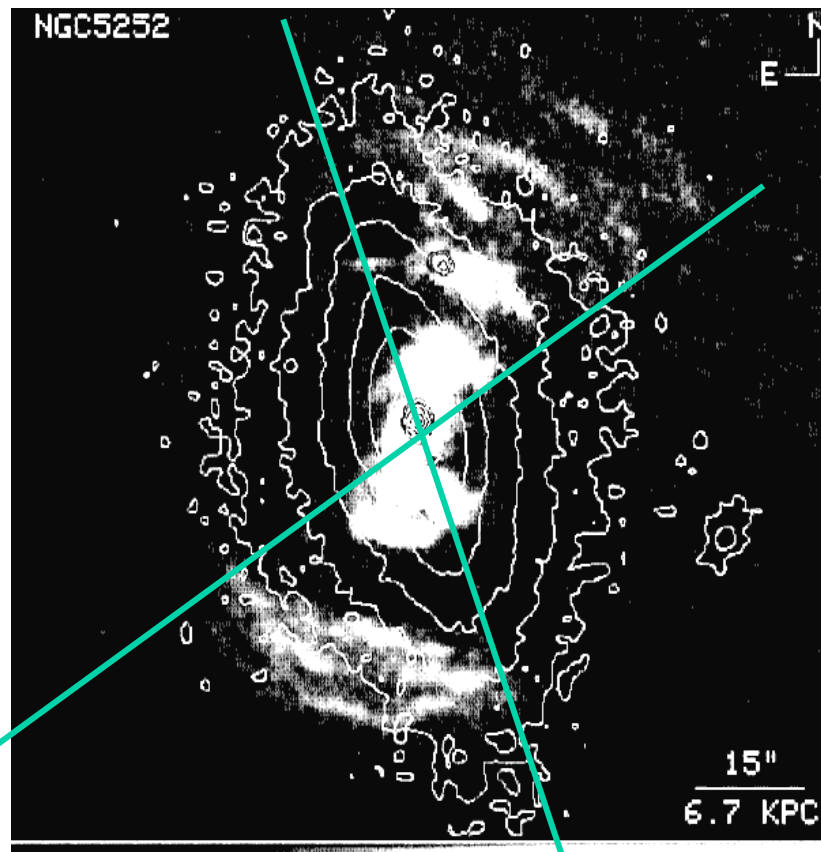
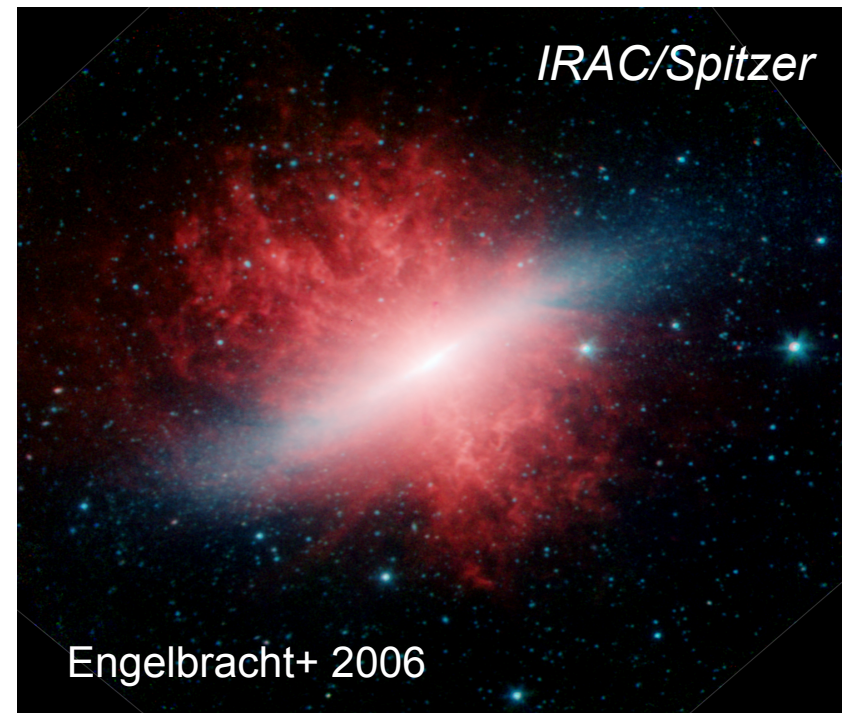
Veilleux+ 2005

A question to the audience:

What timescale is associated with AGN or nuclear \star B activity?

How well can we distinguish them?

Is there a co-dependence?



This calls for a differential study:

Ionization vs. dynamical times in starburst vs. AGN winds

THREE-DIMENSIONAL INTEGRAL FIELD OBSERVATIONS OF 10 GALACTIC WINDS. I. EXTENDED PHASE ($\gtrsim 10$ Myr) OF MASS/ENERGY INJECTION BEFORE THE WIND BLOWS

R. G. SHARP¹ AND J. BLAND-HAWTHORN^{2,3,4}

¹ Anglo-Australian Observatory, P.O. Box 296, Epping, NSW 1710, Australia; rgs@ao.gov.au

² Sydney Institute for Astronomy, School of Physics A28, University of Sydney, NSW 2006, Australia

³ Physics Department, University of Oxford, 1 Keble Rd, Oxford, OX1 3RH, UK; jbh@physics.usyd.edu.au

Received 2009 April 11; accepted 2010 January 25; published 2010 February 18

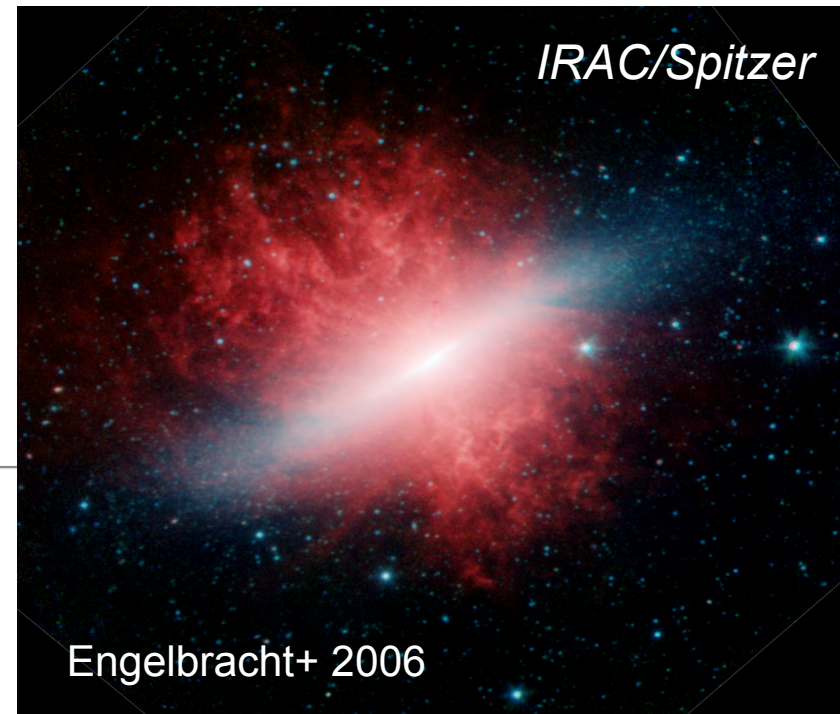
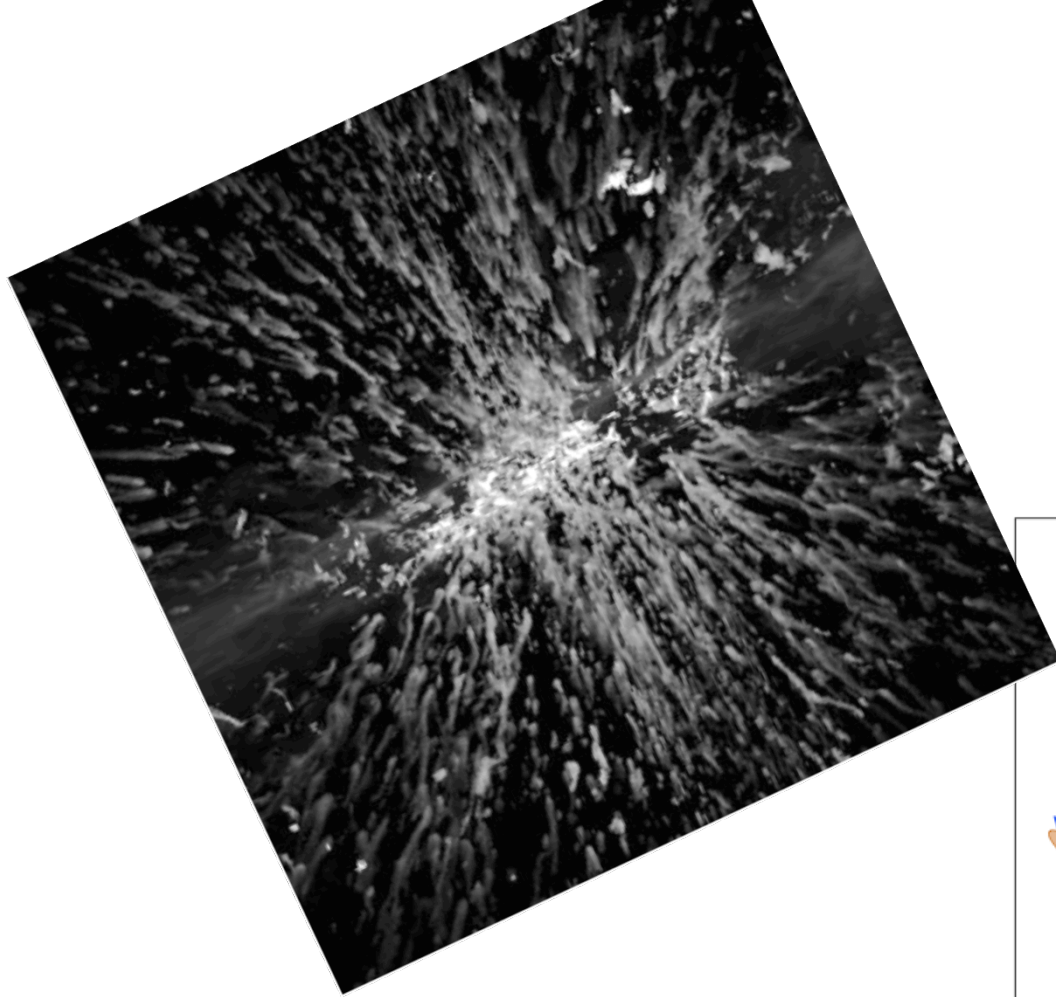
ABSTRACT

In recent years, we have come to recognize the widespread importance of large-scale winds in the life cycle of galaxies. The onset and evolution of a galactic wind is a highly complex process which must be understood if we are to understand how energy and metals are recycled throughout the galaxy and beyond. Here we present three-dimensional spectroscopic observations of a sample of 10 nearby galaxies with the AAOmega-SPIRAL integral-field spectrograph on the 3.9 m Anglo-Australian Telescope, the largest survey of its kind to date. The double-beam spectrograph provides spatial maps in a range of spectral diagnostics: [O III]5007, H β , Mg *b*, Na D, [O I]6300, H α , [N II]6583, [S II]6717, 6731. We demonstrate that these flows can often separate into highly ordered structures through the use of ionization diagnostics and kinematics. All of the objects in our survey show extensive wind-driven filamentation along the minor axis, in addition to large-scale disk rotation. Our sample can be divided into either starburst galaxies or active galactic nuclei (AGNs), although some objects appear to be a combination of these. The total ionizing photon budget available to both classes of galaxies is sufficient to ionize all of the wind-blown filamentation out to large radius. We find, however, that while AGN photoionization always dominates in the wind filaments, this is not the case in starburst galaxies where shock ionization dominates. This clearly indicates that after the onset of star formation, there is a substantial delay ($\gtrsim 10$ Myr) before a starburst wind develops. We show why this behavior is expected by deriving “ionization” and dynamical timescales for both AGNs and starbursts. We establish a sequence of events that lead to the onset of a galactic wind. The clear signature provided by the ionization timescale is arguably the strongest evidence yet that the starburst phenomenon is an impulsive event. A well-defined ionization timescale is not expected in galaxies with a protracted history of circumnuclear star formation. Our three-dimensional data provide important templates for comparisons with high-redshift galaxies.

Key words: galaxies: individual (NGC 253, NGC 1365, NGC 1482, NGC 1808, NGC 3628, NGC 5128, Circinus, NGC 6240, NGC 6810, IC 5063)

Online-only material: color figures

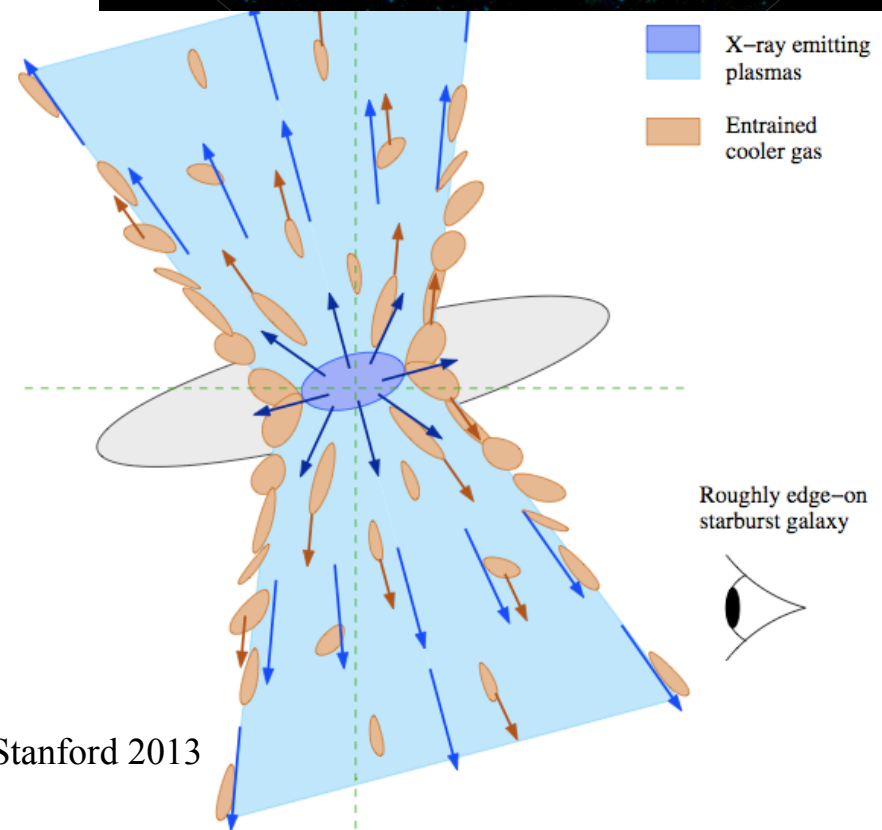
KIPAC Stanford 2013



Origin & physics of filaments:

Shoppell & JBH 1998; Greve 2004
J. Cooper+ 2008, 2009

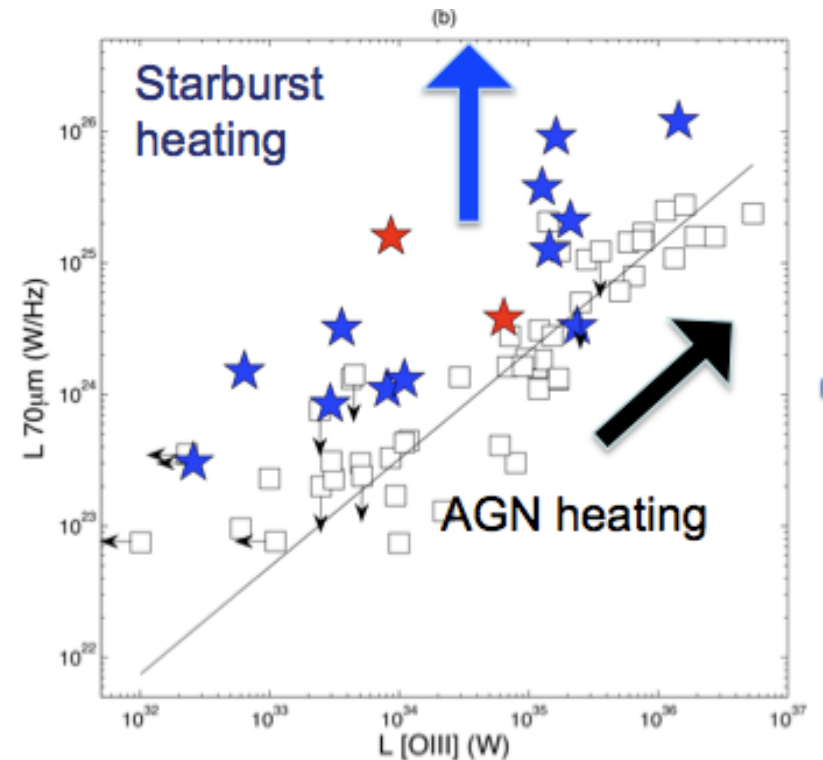
Rotation in the filament system
tells you all the gas you see is
entrained from the disk.



It is surprisingly difficult to distinguish the large-scale energetic influence of an AGN vs. ★B:

1. Both operate on similar timescales?
2. Both have similar photon budgets scaled to L_{BOL}
3. Both generate powerful outflows
4. Both heat circumnuclear dust

Dan Dicken



Ionizing photon budget from AGN

$$L_A = \epsilon \dot{m} c^2 \quad (1)$$

$$= 7 \times 10^{11} \left(\frac{\epsilon}{0.05} \right) \left(\frac{\dot{m}}{M_\odot \text{ yr}^{-1}} \right) L_\odot \quad (2)$$

$$L_E = \frac{4\pi G m_{\text{BH}} m_p c}{\sigma_T}$$
$$= 2 \times 10^{11} \left(\frac{m_{\text{BH}}}{10^7 M_\odot} \right) L_\odot$$

$$\mathcal{N}_{\text{LyC,A}} \sim 10^{54} \xi_A \left(\frac{L_{\text{bol,A}}}{10^{11} L_\odot} \right) \text{ phot s}^{-1}$$

Ionizing photon budget from nuclear ★B

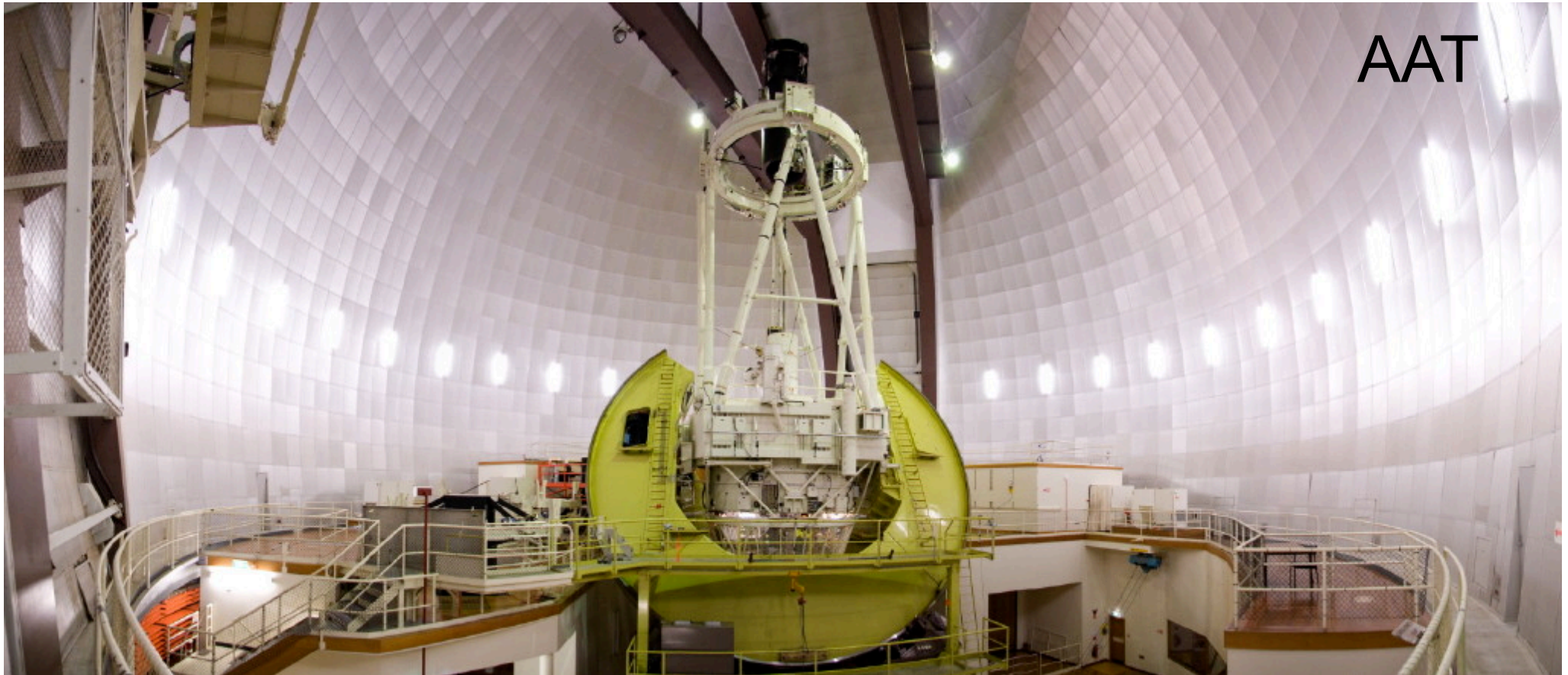
$$L_S \sim 10^{11} \left(\frac{\dot{s}}{5 M_\odot \text{ yr}^{-1}} \right) \left(\frac{\Delta t}{10^8 \text{ yr}} \right)^{0.67} \\ \times \left(\frac{m_L}{1 M_\odot} \right)^{0.23} \left(\frac{m_U}{100 M_\odot} \right)^{0.37} L_\odot$$

$$\dot{s} \sim 5 \left(\frac{L_S}{10^{11} L_\odot} \right) \left(\frac{\Delta t}{10^8 \text{ yr}} \right)^{-0.67} M_\odot \text{ yr}^{-1}.$$

$$\mathcal{N}_{\text{LyC,S}} \sim 10^{54} \left(\frac{\dot{s}}{5 M_\odot \text{ yr}^{-1}} \right) \left(\frac{m_L}{1 M_\odot} \right)^{0.23} \left(\frac{m_U}{100 M_\odot} \right)^{0.37} \\ \sim 10^{54} \xi_S \left(\frac{L_{\text{bol}}}{10^{11} L_\odot} \right) \text{ phot s}^{-1}$$

SPIRAL: optical integral field dual-beam spectroscopy

- A sample of nearby AGN and ★B wind galaxies
- Luminosity range: $1-10 \times 10^{10} L_{\odot}$
- Most AGNs show evidence of circumnuclear SF



KIPAC Stanford 2013

AAOmega+SPIRAL

- **Dual beam spectrograph**
- 512 element fibre feed (now x2)
- 32x16 rectangular array (now 32x32)
- **0.7 arcsec square pixels**
- 11.2x22.4 arcsec FoV (now 22.4x22.4)
- $R = 5700-6300$ over 370-890 nm

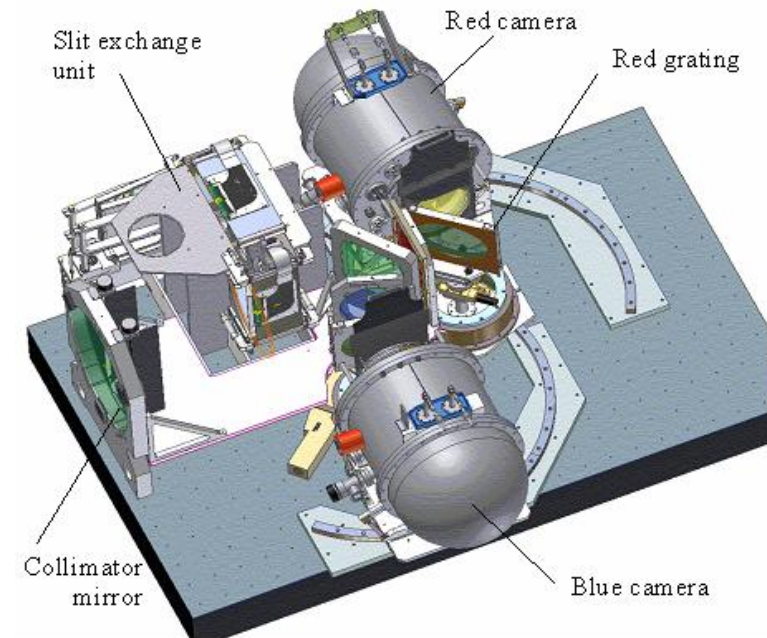
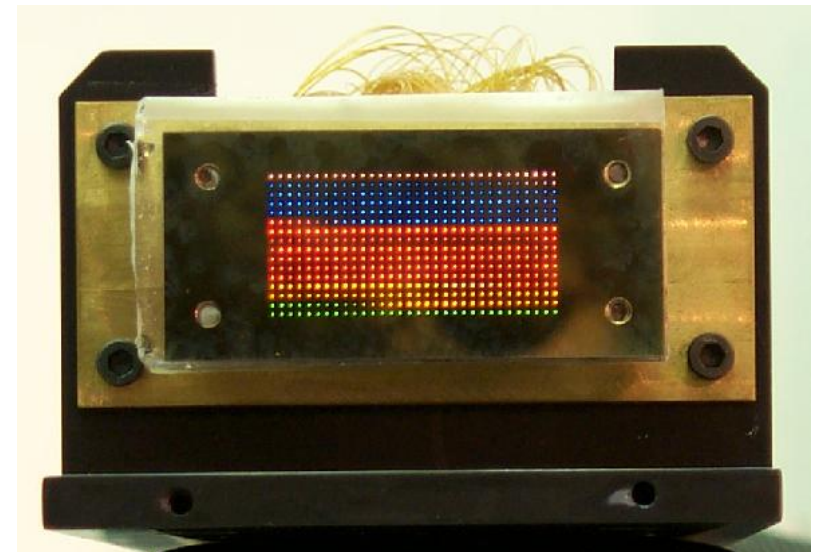
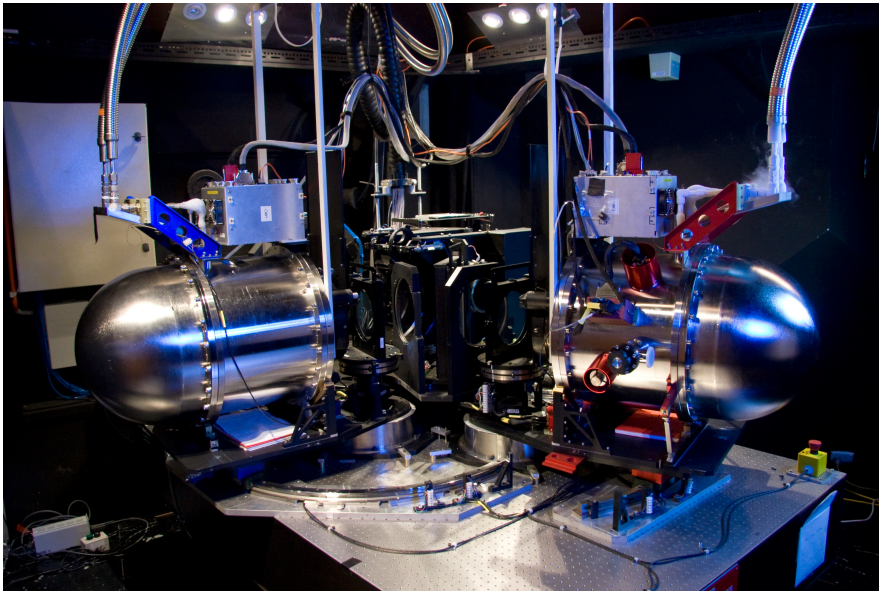


Figure 1. Physical layout of AAOmega, layout, showing the red camera in high dispersion mode, and blue camera in low dispersion mode.



Only sources with known outflows were chosen

Object	RA/Dec (J2000)	Redshift	Hubble type ¹	Spec class ²	i	M _B	L _{Bol} ³
NGC 253	00 47.6 −25 18	0.00081	Sc(X)	HII	86	−20.02	2.8
NGC 1365	03 33.7 −36 08	0.00546	Sb(B)	HII, Sy2	63	−21.26	9.3
NGC 1482	03 54.7 −20 30	0.00639	Sa(P)	HII	58	−18.89	1.1
NGC 1808	05 07.7 −37 31	0.00332	SO/a(X)	HII, Sy2?	50	−19.52	2.2
NGC 3628	11 20.3 +13 37	0.00281	Sb(P)	HII, LINER	87	−19.96	2.8
NGC 5128	13 25.3 −43 01	0.00183	SO, Lenticular	Sy2	43	−20.97	8.5
Circinus	14 13.2 −65 20	0.00145	Sb(A)	Sy2	65	−21.23	9.0
NGC 6240	16 53.0 +02 24	0.02445	I0	LINER, Sy2	—	−21.30	8.2
NGC 6810	19 43.6 −58 40	0.00678	Sa(A)	HII, Sy2?	82	−20.61	5.5
IC 5063	20 52.0 −57 04	0.01135	Sa	Sy2	—	−20.34	4.2

AGNs are 3x more luminous than ★B on average

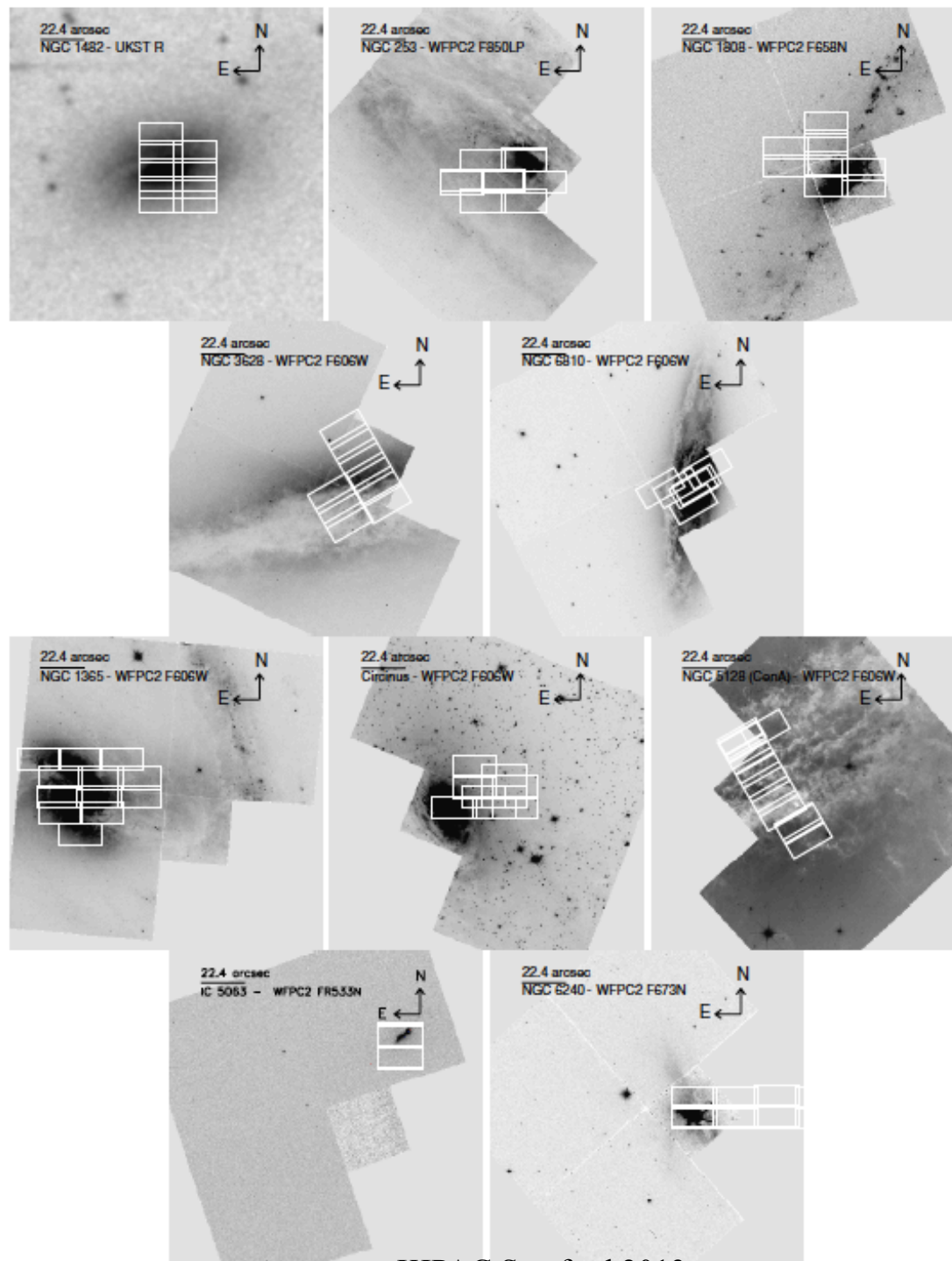


Figure 1. SPIRAL IFU footprints. Images are taken from *HST*/WFPC2 associations where available and from the DSS for NGC 1482. The 22.4 long axis of the SPIRAL IFU is indicated for scale. Note the unusual P.A. for observations of NGC 6810, NGC 3628, and NGC 5128 due to the detailed requirements of the NGC 5128 observing program during the 2007 May run.

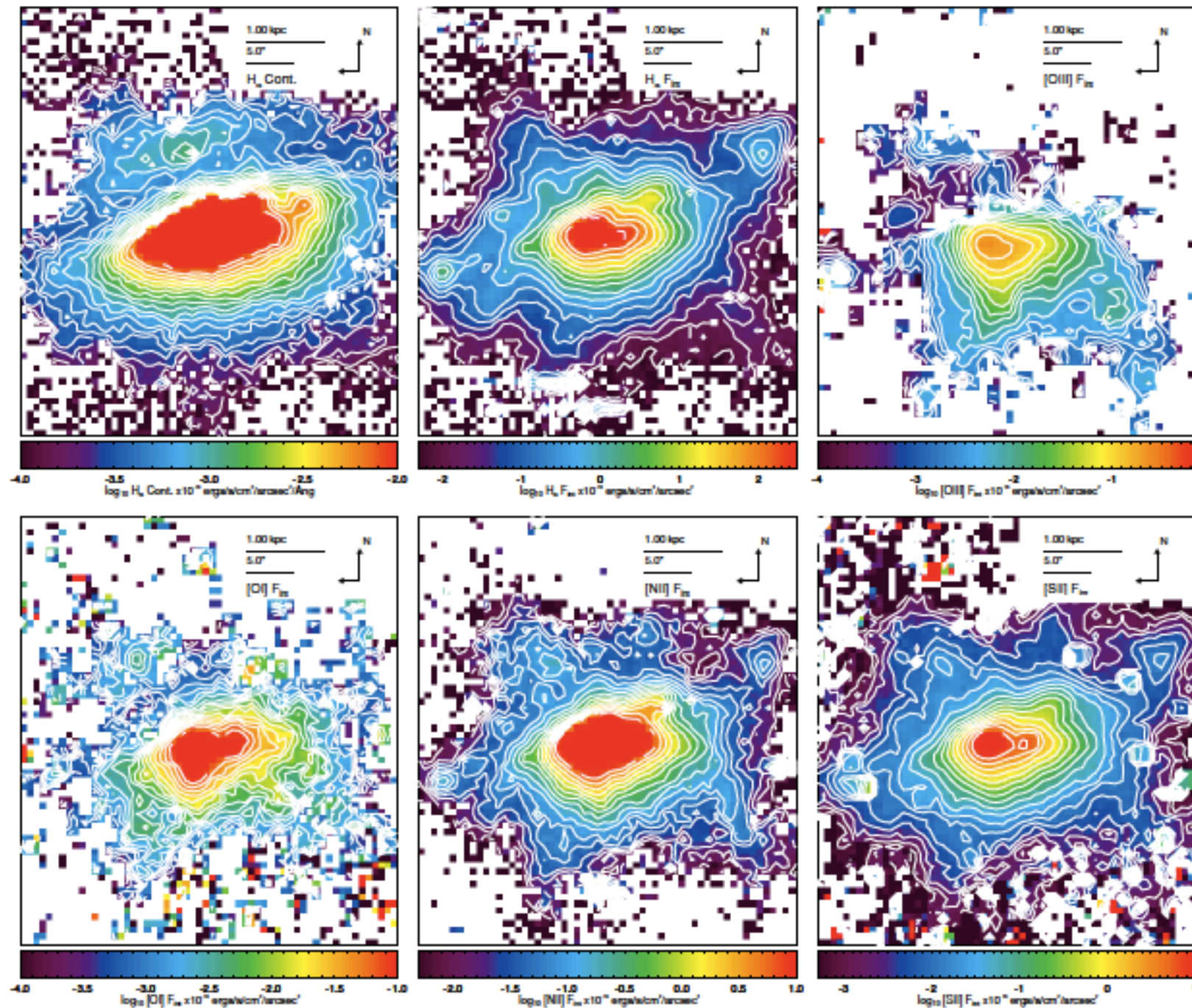
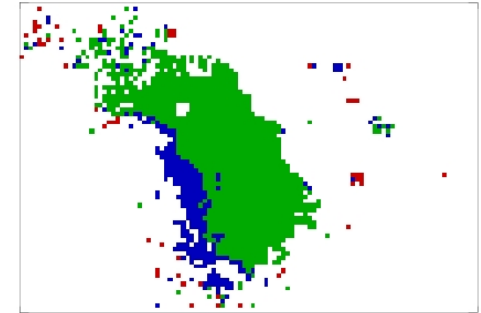
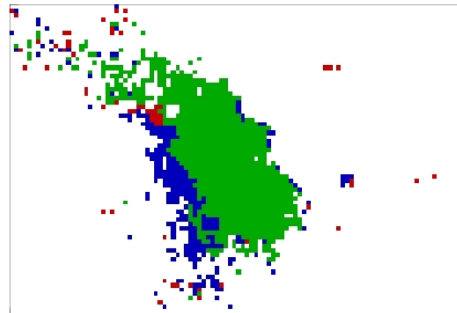
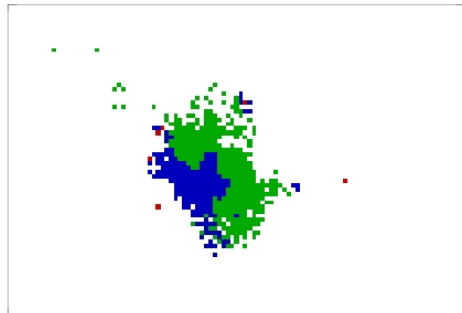
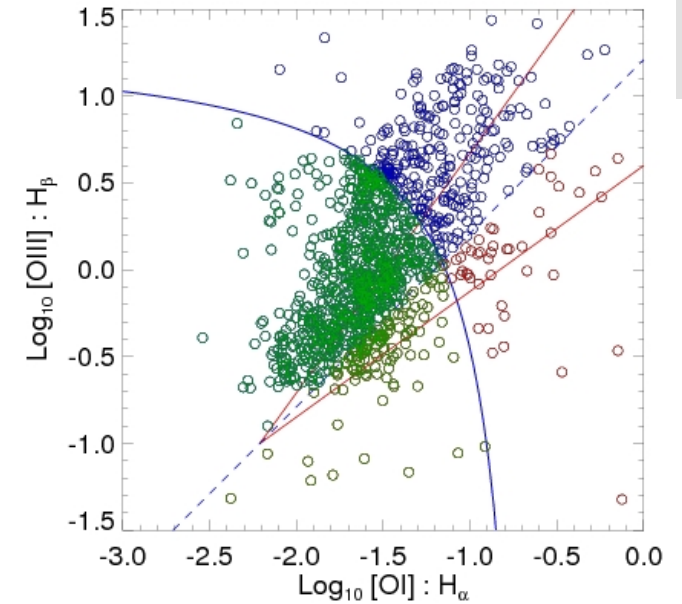
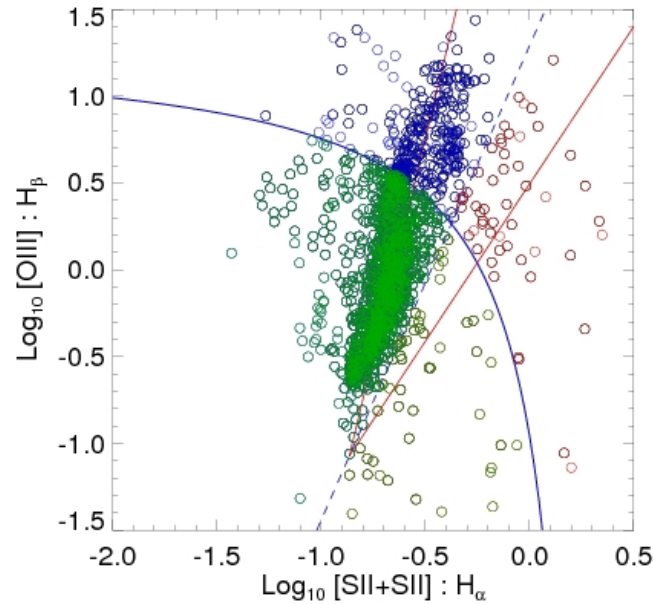
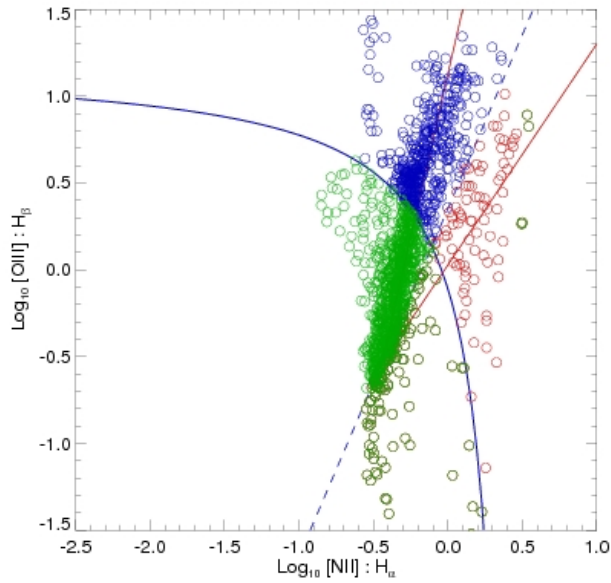
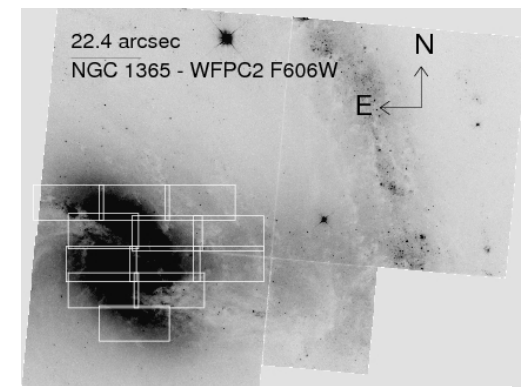


Figure 2. NGC 1482: emission-line integrated flux maps are generated by single Gaussian fitting to individual spectra. The maps shown (left to right, top to bottom) are the continuum at line center for $H\alpha$ followed by integrated intensity maps (F_{int}) for $H\alpha$, $[O III] \lambda 6300$, $[N II] \lambda 6583$, and $[S II] \lambda 6716$. Pixels for which no valid fit was obtained are left blank.

(A color version of this figure is available in the online journal.)

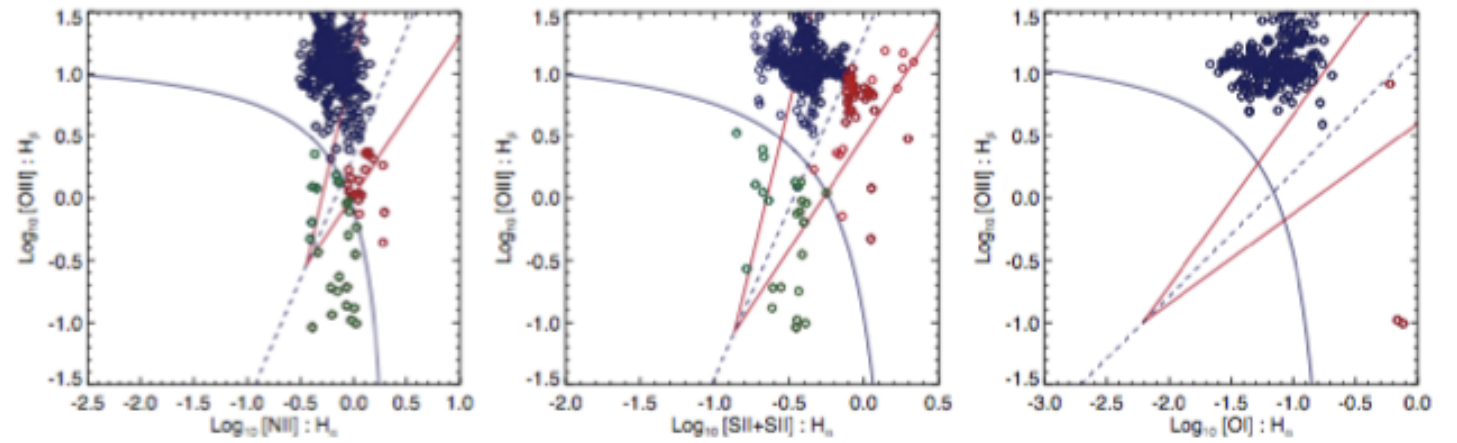
Example 1. AGN: NGC 1365

Indicative of the full AGN sample

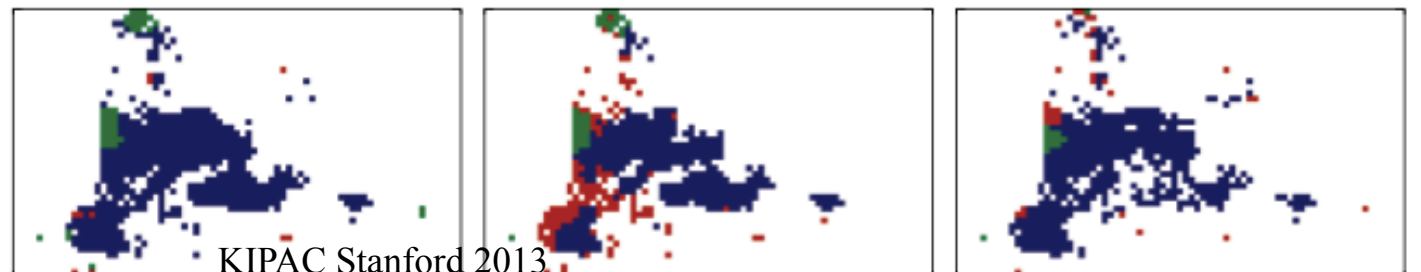
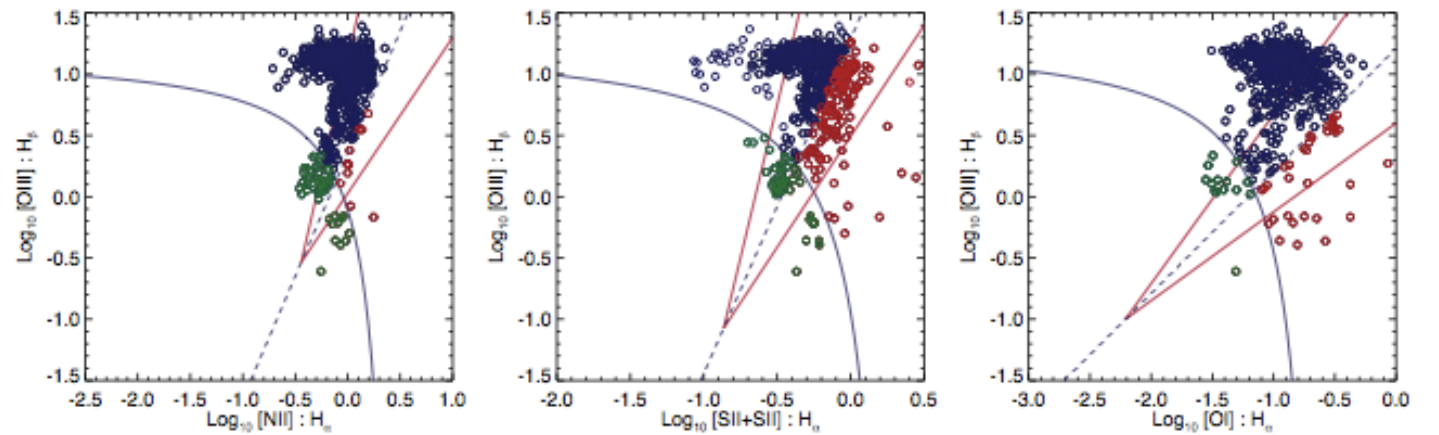


Off planer gas is photoionised by a hard spectrum source (AGN)

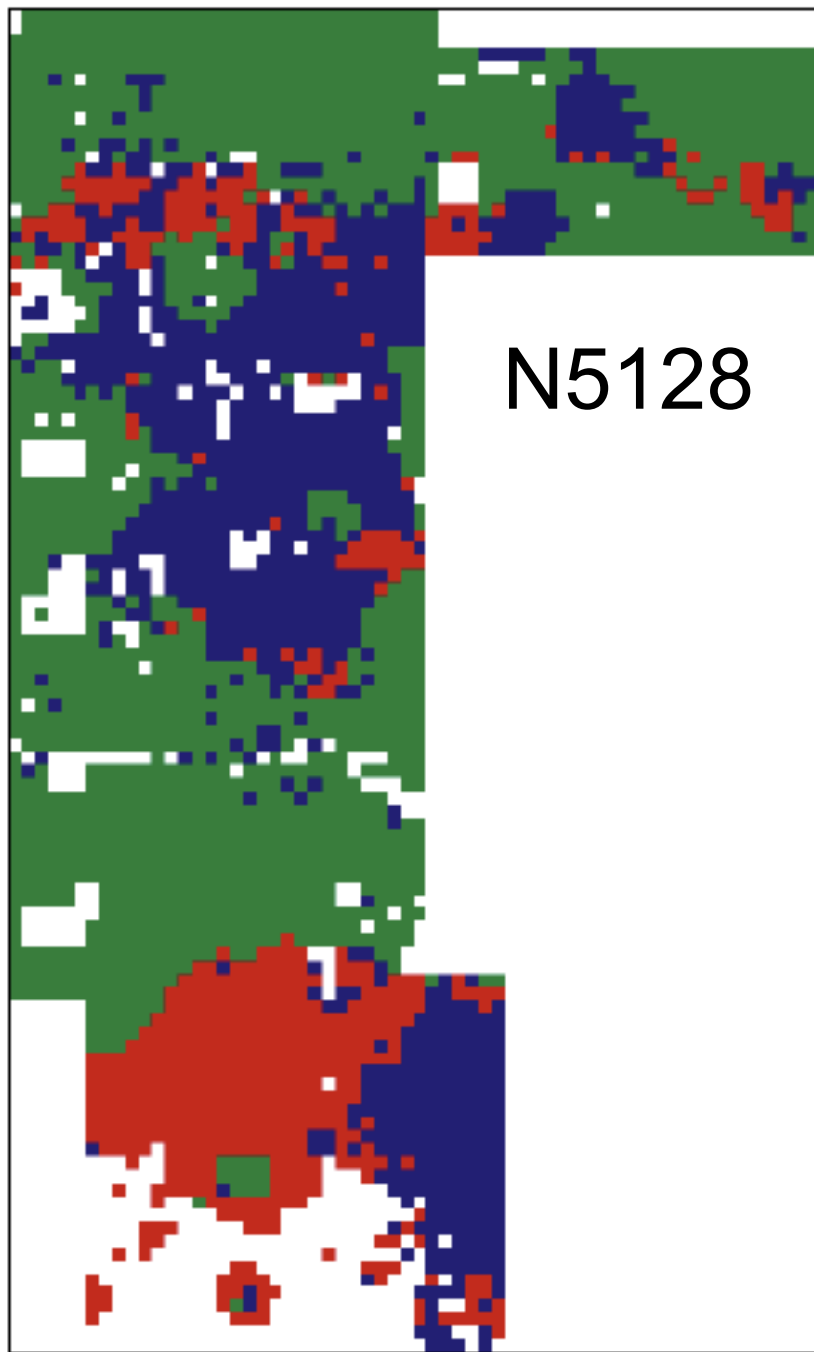
AGN: IC 5063



AGN: Circinus



AGN ionisation cones: several recovered, one new



N5128

N1365

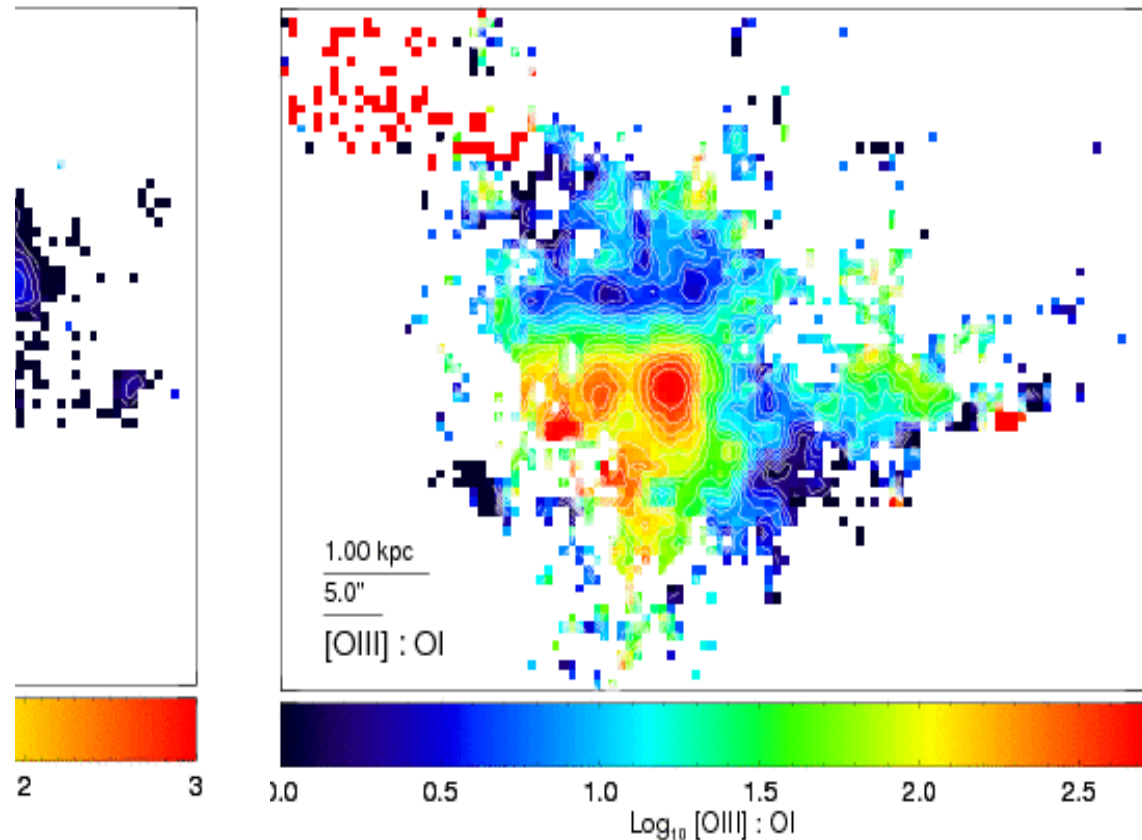


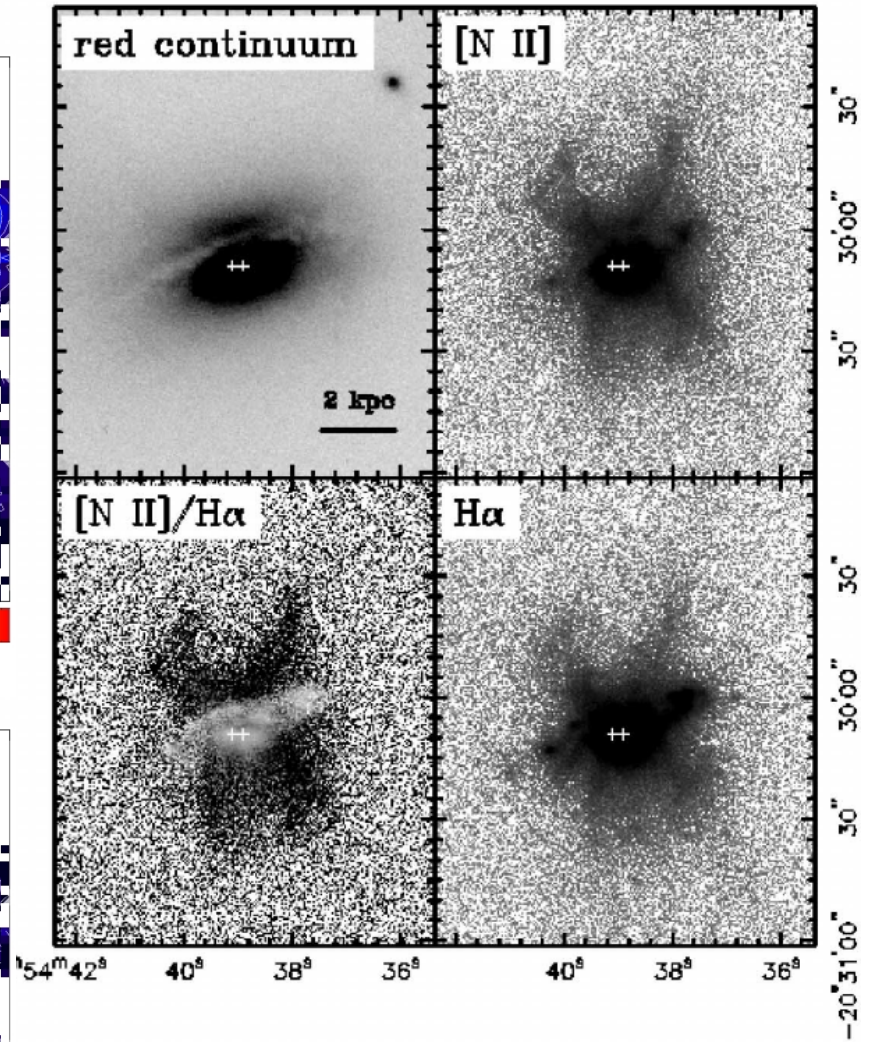
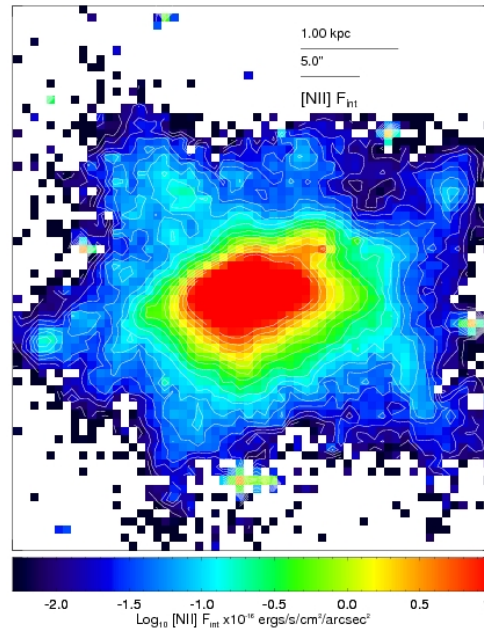
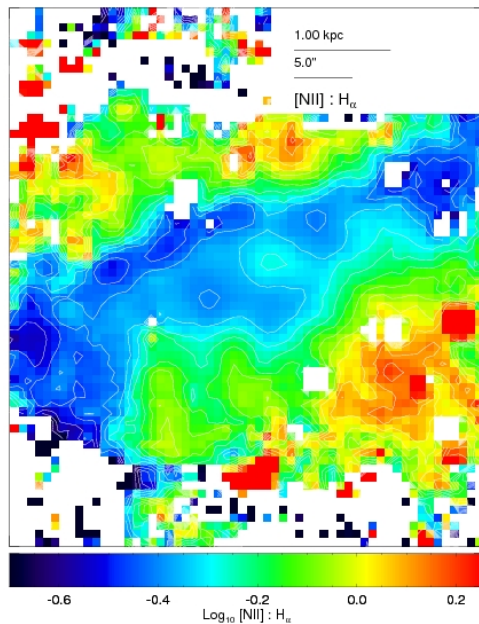
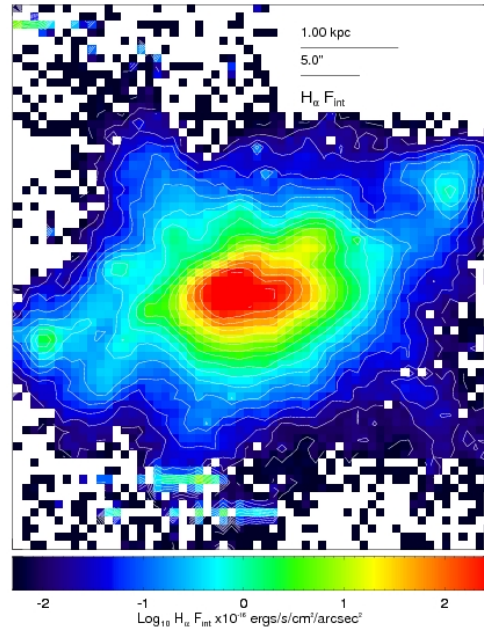
Figure 25. NGC 5128 (CenA): the ionization cone due to the hard AGN spectrum is revealed more clearly in the data after spatially re-binning the spectra 3×3 . The classification scheme from the $[\text{O III}]/\text{H}\beta$ vs. $[\text{N II}]/\text{H}\alpha$ IDD (Figure 24) is repeated here.

(A color version of this figure is available in the online journal.)

Example 2. ★B: NGC 1482

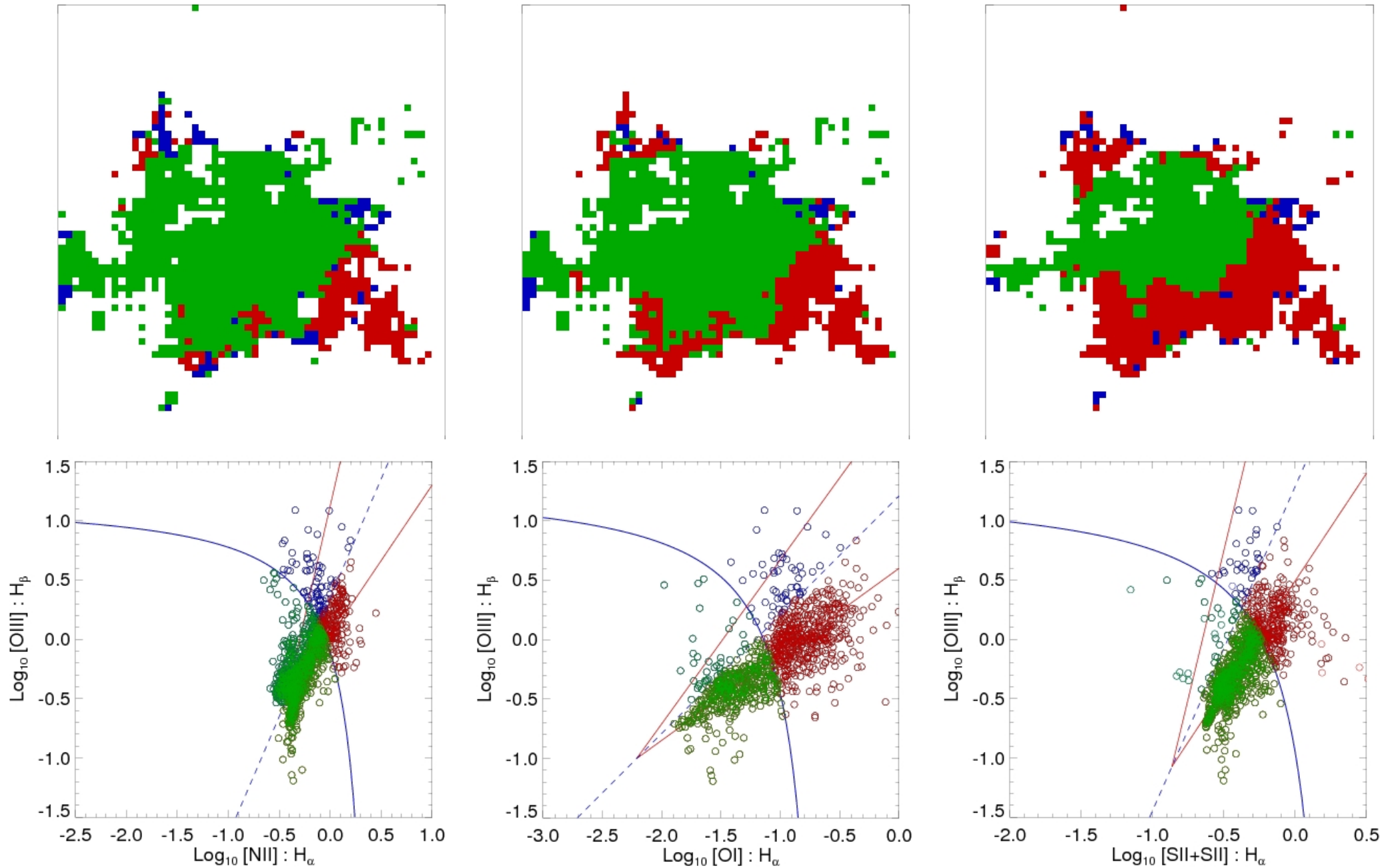
No evidence for an AGN
across multiple frequencies

Indicative of full
starburst sample



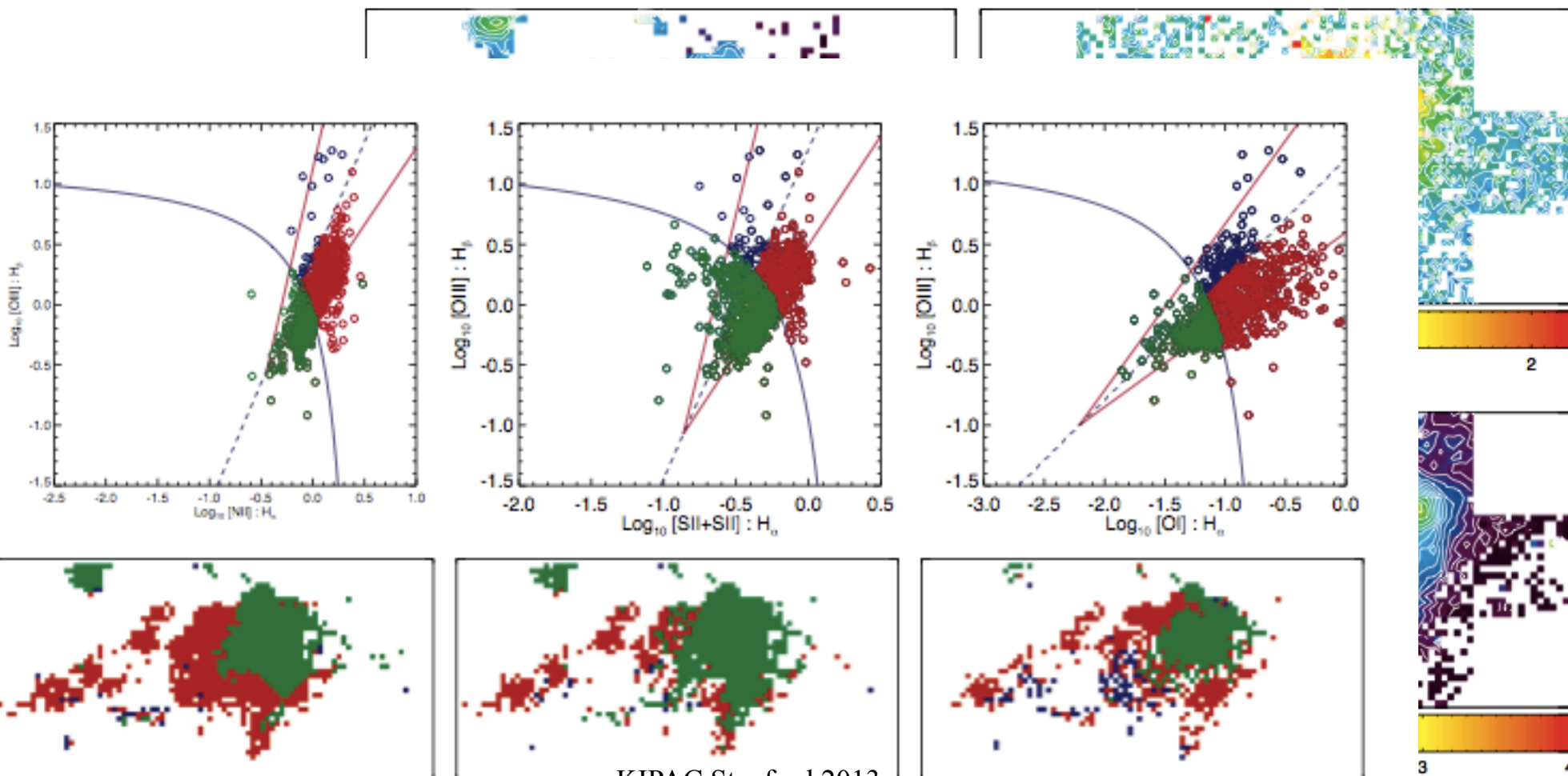
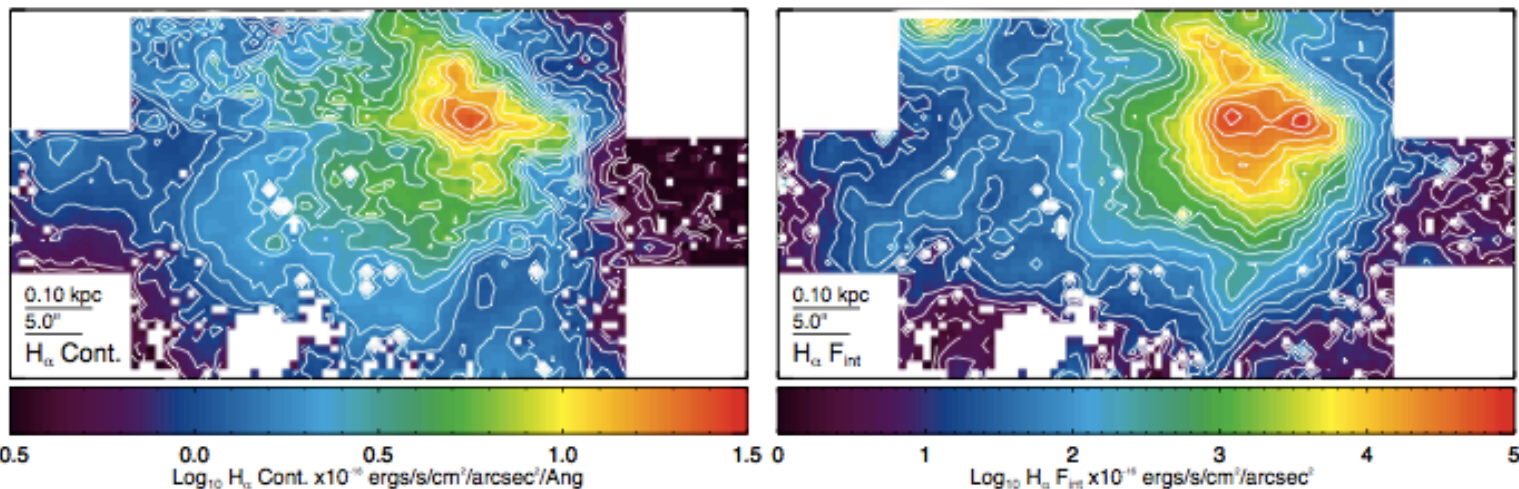
AAT/TTF Veilleux &
Rupke 2002
Shocked gas excitation?

Ionisation Diagnostic Diagrams



Confirming **shocks** as the most likely excitation mechanism above the disk plane

★B: NGC 253



Far off the plane:

AGN winds are
photo-ionized

★B winds are
shock-ionized

Object	L_{Bol} ($10^{10} L_{\odot}$)	Extent (arcsec)	Deprojected (kpc)	$\mu(\text{H}\alpha)$ @ 1 kpc
NGC 253	2.8	30.5	0.5	$3.8\text{e-}16 \pm 4.6\text{e-}16$
NGC 1365	9.3	16.4	1.8	$2.6\text{e-}16 \pm 1.2\text{e-}16$
NGC 1482	1.1	15.5	2.2	$8.9\text{e-}16 \pm 4.4\text{e-}16$
NGC 1808	2.2	22.5	1.7	$1.6\text{e-}16 \pm 5.1\text{e-}17$
NGC 3628	2.8	28.0	0.4	$5.2\text{e-}17 \pm 2.2\text{e-}17$
NGC 5128	8.5	36.0	2.8	$4.7\text{e-}16 \pm 2.2\text{e-}16$
Circinus	9.0	24.6	0.4	$1.9\text{e-}16 \pm 8.5\text{e-}17$
NGC 6810	5.5	12.0	16.4	$5.5\text{e-}16 \pm 2.4\text{e-}16$
IC 5063	4.2	6.0	1.4	$1.3\text{e-}15 \pm 5.3\text{e-}16$

This holds for either AGN or ★B ionization

$$\mu(\text{H}\alpha) = 1 \times 10^{-14} \left(\frac{r}{1 \text{ kpc}} \right)^{-2} \left(\frac{L_{\text{bol}}}{10^{11} L_{\odot}} \right) \text{ cgs}$$

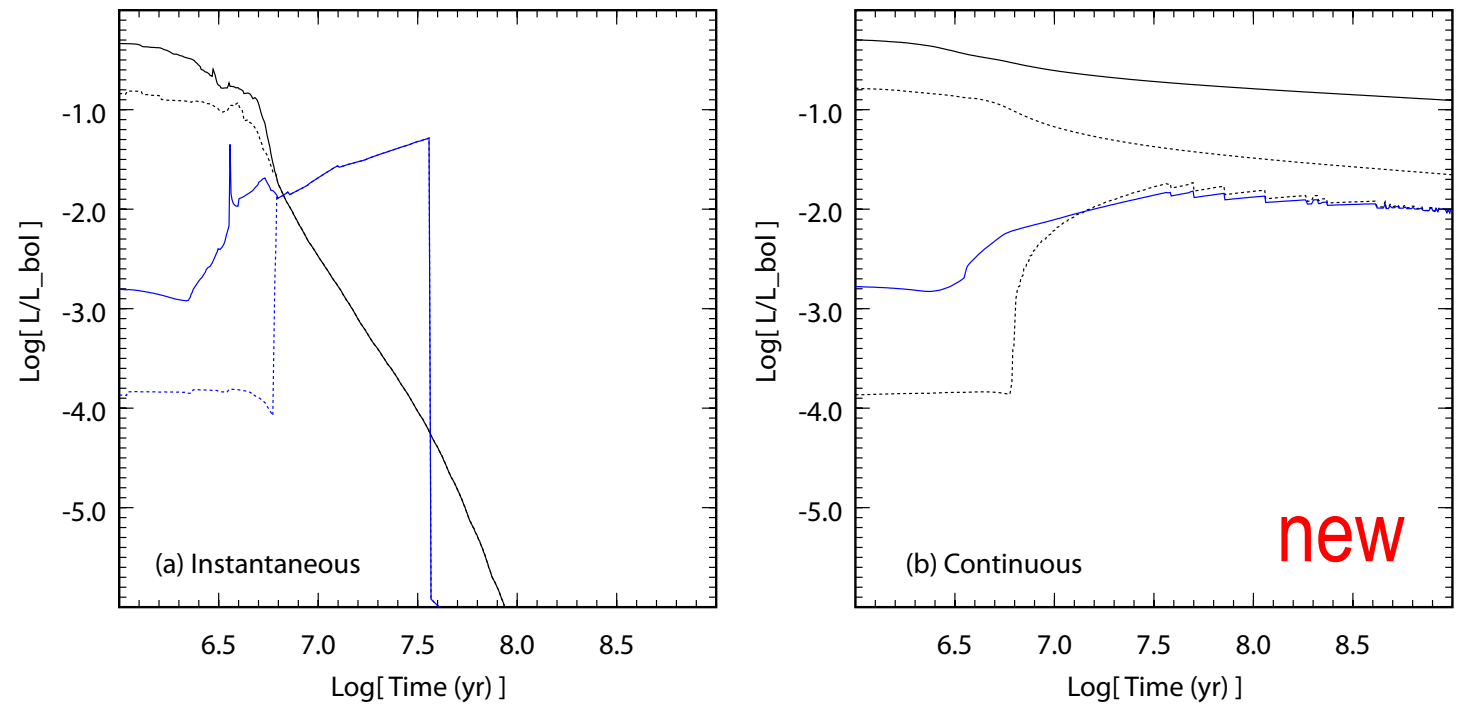
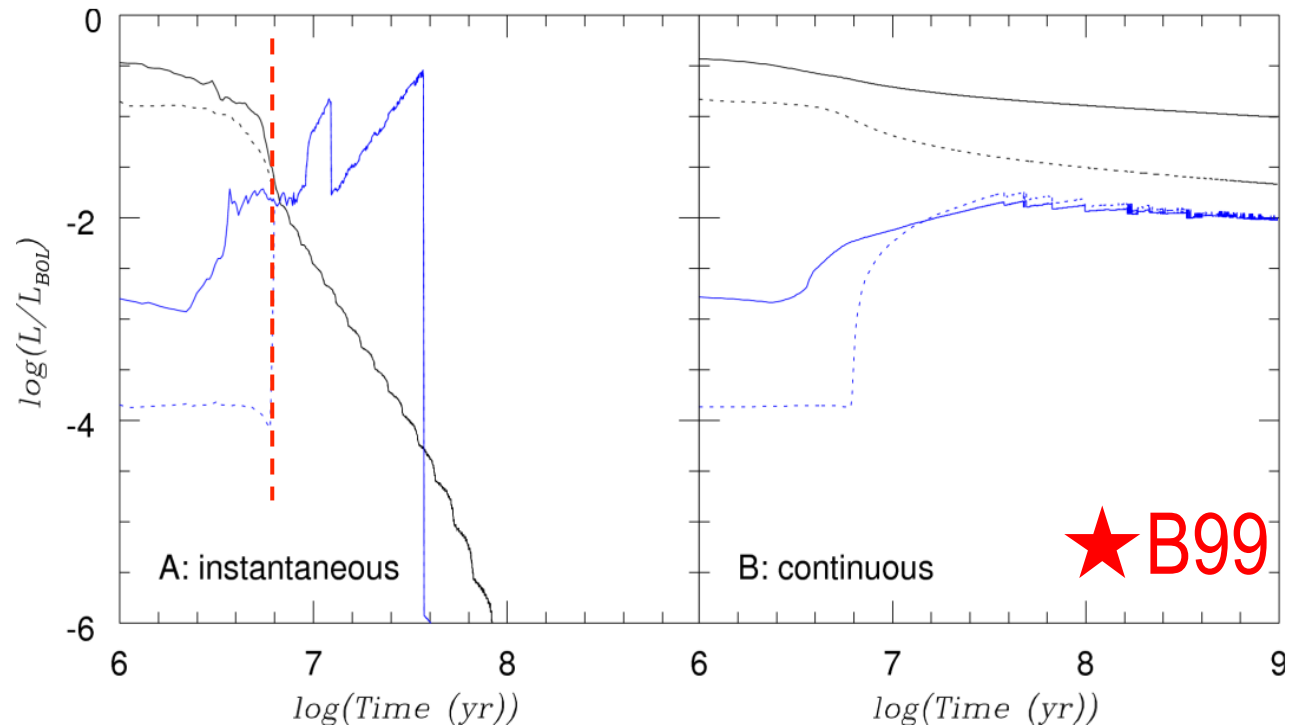
Shock ionization

$$\mu_{\text{shock}}(\text{H}\alpha) \approx 5 \times 10^{-16} \left(\frac{V_{\text{shock}}}{100 \text{ km s}^{-1}} \right)^{2.4} \left(\frac{n_o}{10 \text{ cm}^{-3}} \right) \text{ cgs} \quad (25)$$

So even though ★B and AGN have the same UV budget for the same L_{BOL} , stellar photoionization is never seen (except for emission close to the plane)

★B phenomenon is impulsive

★B wind blows after initial delay > 10 Myr



Sequence of events:

1. Massive stars born in dense clouds



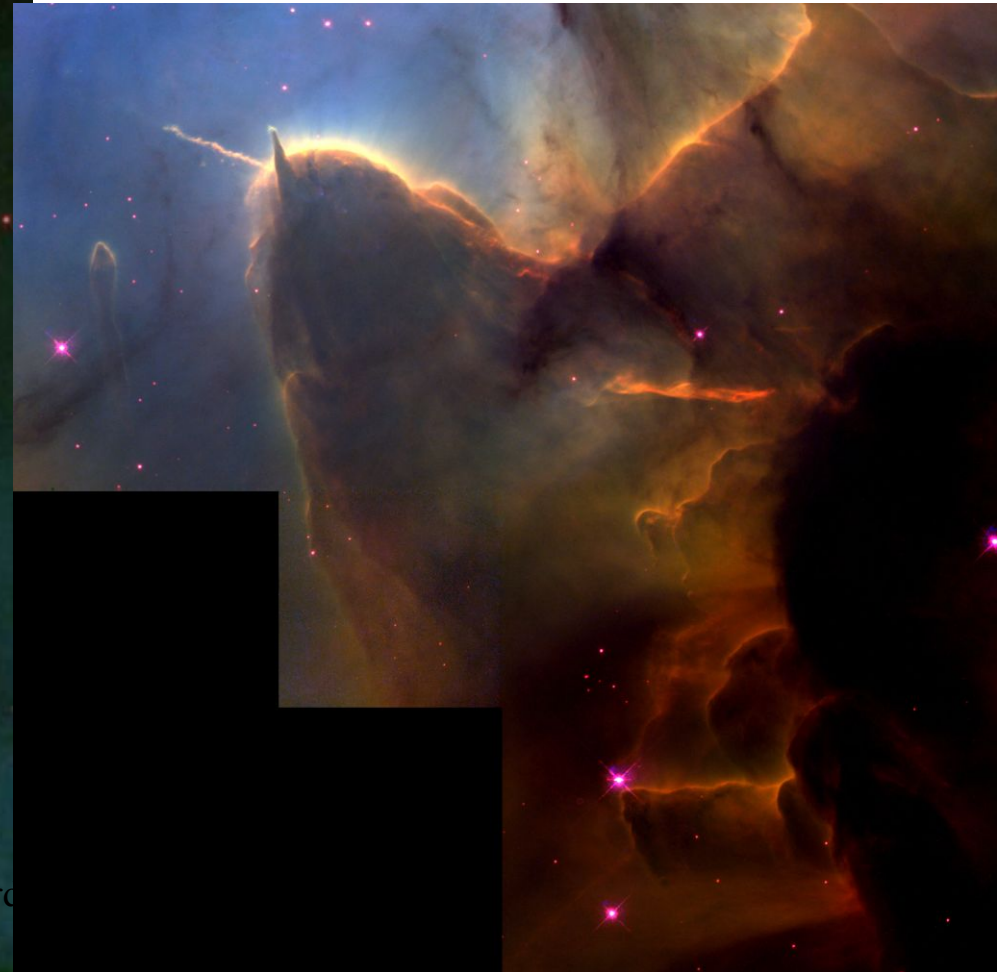
Sequence of events:

2. Massive stars ionize
intracloud medium and
evaporate cloud surfaces



Hot young stars ionize the skins of dense clouds:

We need the evaporated material before the onset of a large-scale wind.



Sequence of events:

2. Massive stars ionize
intracloud medium and
evaporate cloud surfaces



Sequence of events:

3. O stars go supernova!



Sequence of events:

4. SNe heat the diffuse gas



Sequence of events:

5. UV intensity plummets
(since $\geq 13M_{\odot}$ have gone!)



Sequence of events:

6. Hot wind escapes



AGN: why is the wind in synchrony with the UV?



energy release rate in a Keplerian disk $\sim GM_{\text{BH}}\dot{m}/2r$

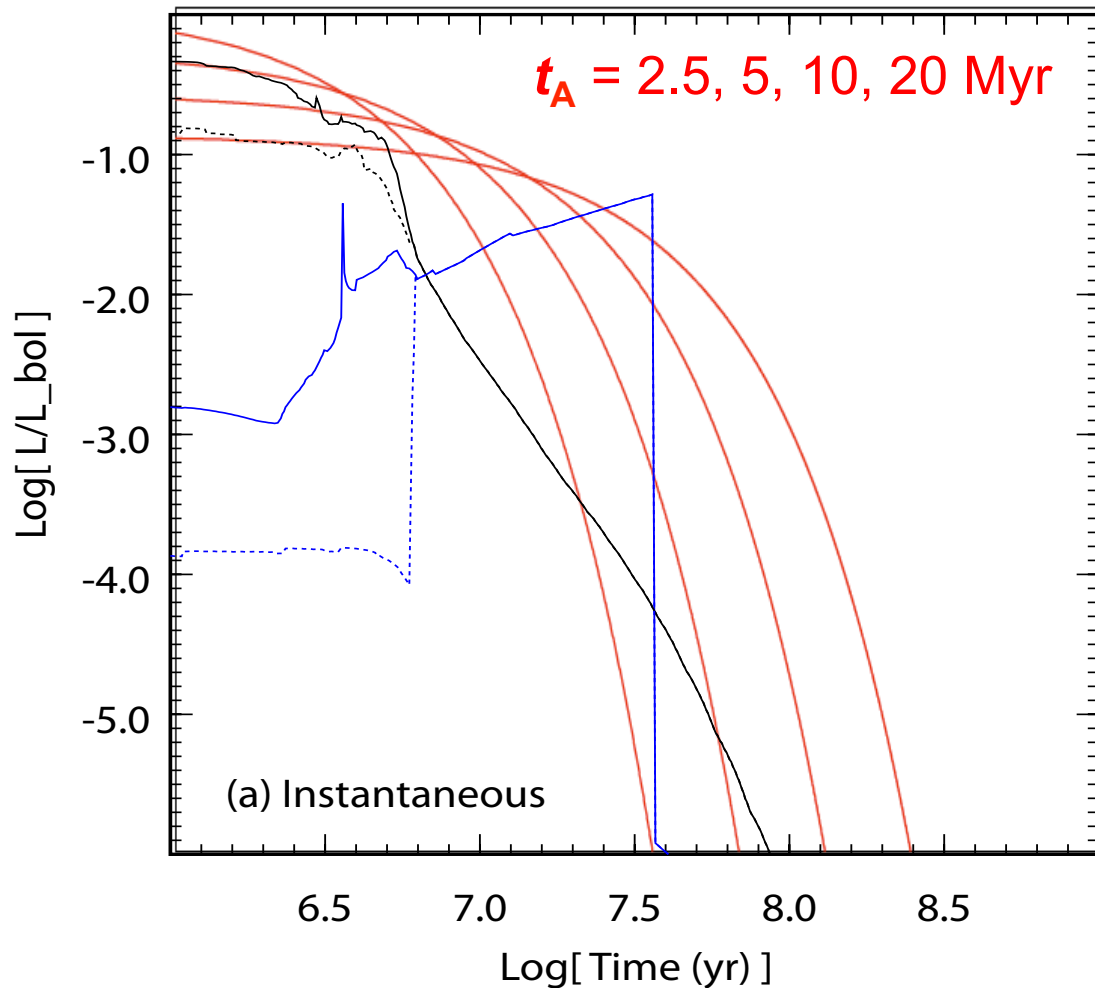
important to balance local flux to local Eddington flux $\sim cGM_{\text{BH}}z/\kappa(r^2+z^2)^{3/2}$

accrete gas inwards until local super-Eddington emissivity reached

AGN result:

There are **few** accretion disk predictions, steady state or otherwise, on the simultaneous presence of jets, winds, cones.

AGN timescale t_A is **long** if wind evolution is much like ★B to avoid dominance of shock ionization.



Colour code:

★B photoionization

★B mechanical

AGN photoionization

AGN normalization:

$$L_A/L_{\text{bol}} = C_{A,\text{max}} \exp(-t/t_A)$$

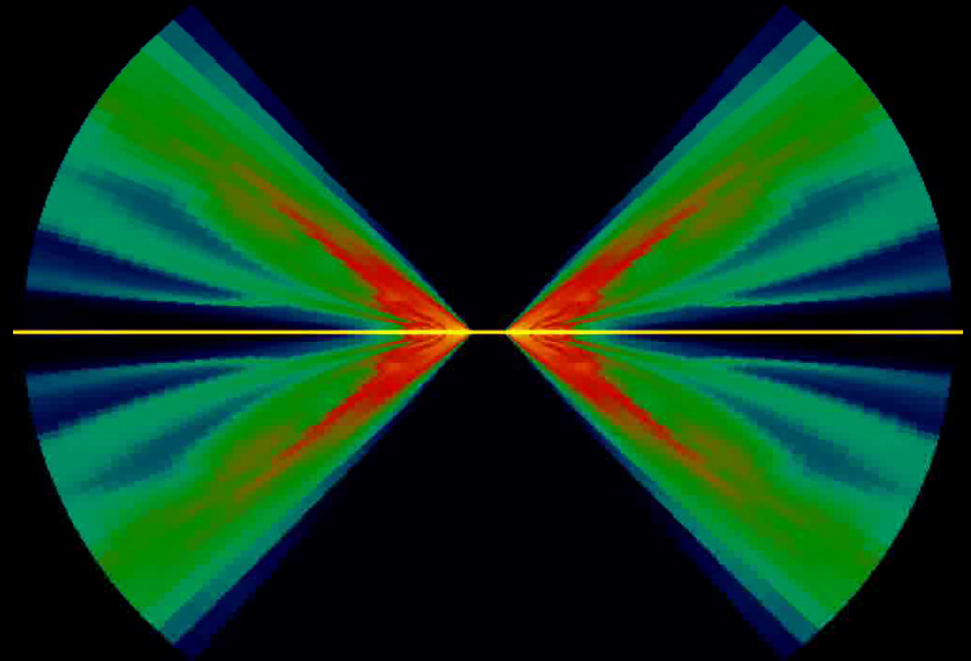
$$\int_{\text{LL}}^{\infty} \frac{L_A}{h\nu} d\nu = \mathcal{N}_{\text{LyC},A}$$

Proga & Kallman (2004)

With no x-rays



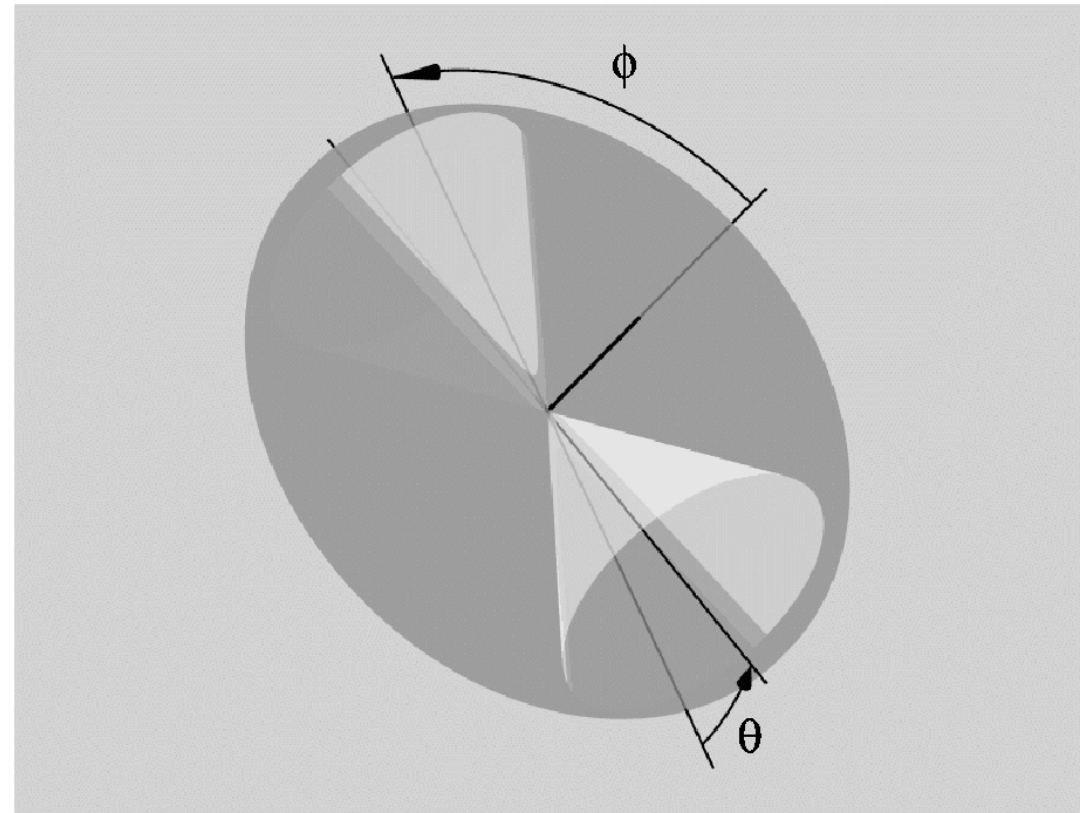
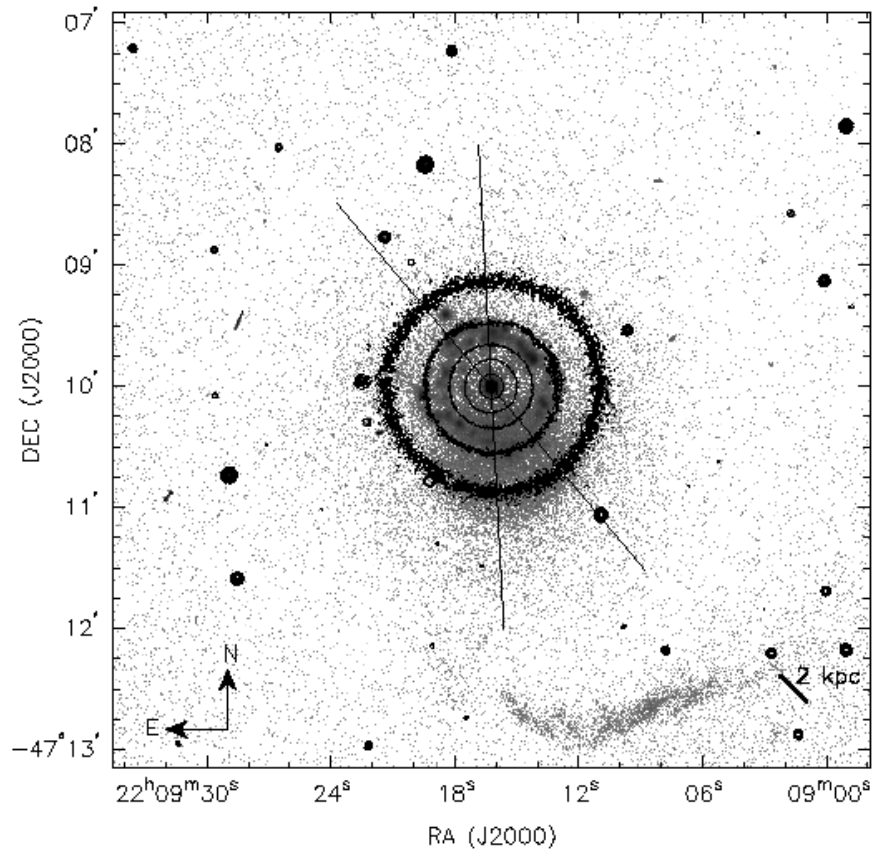
With x-rays



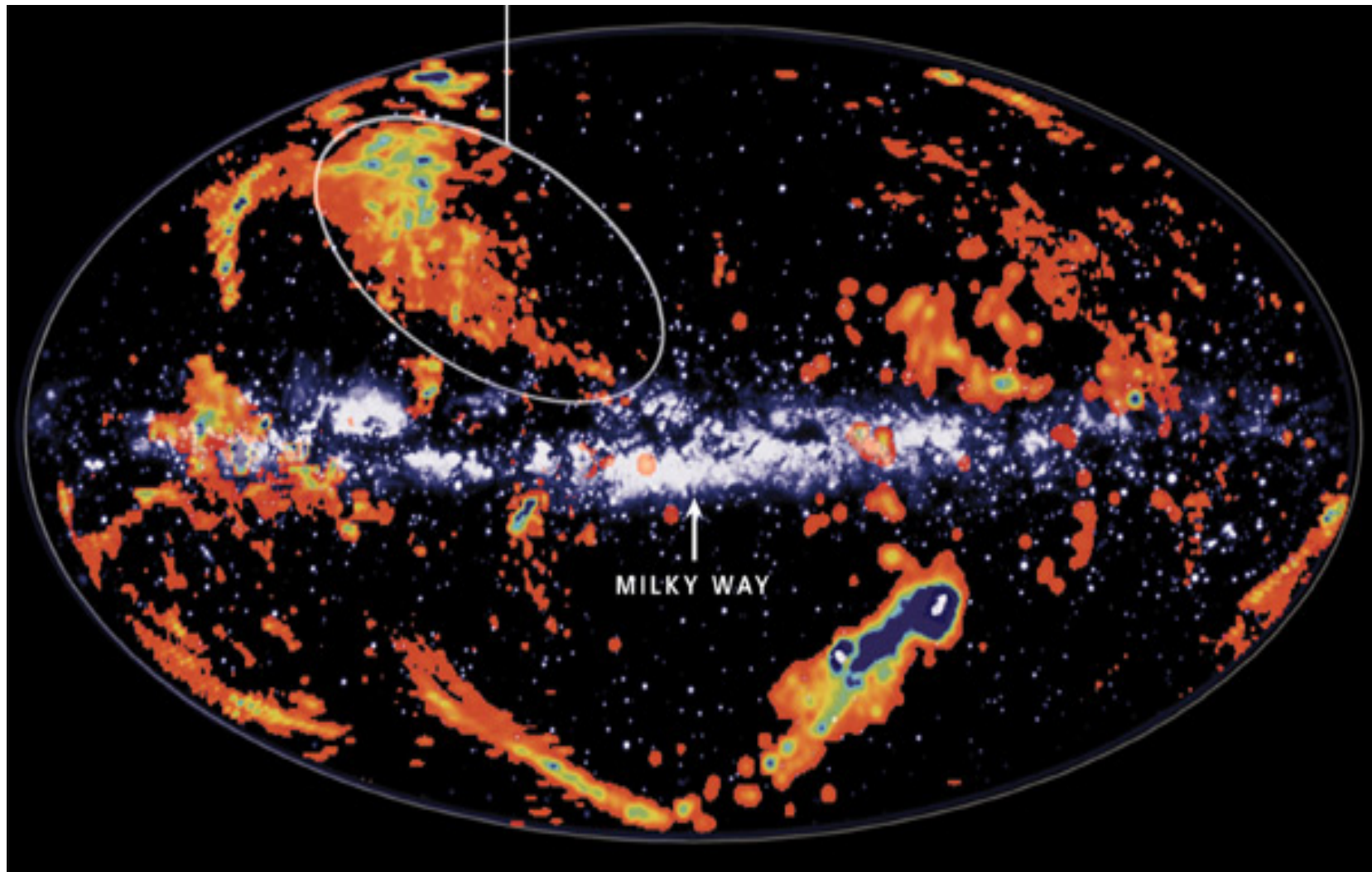
They find that $M_{\text{BH}} \sim 4 \times 10^6 M_{\odot}$ must be close to $f_E \sim 1$ to have any chance of launching a wind (but this can be much less in $10^8 M_{\odot}$)

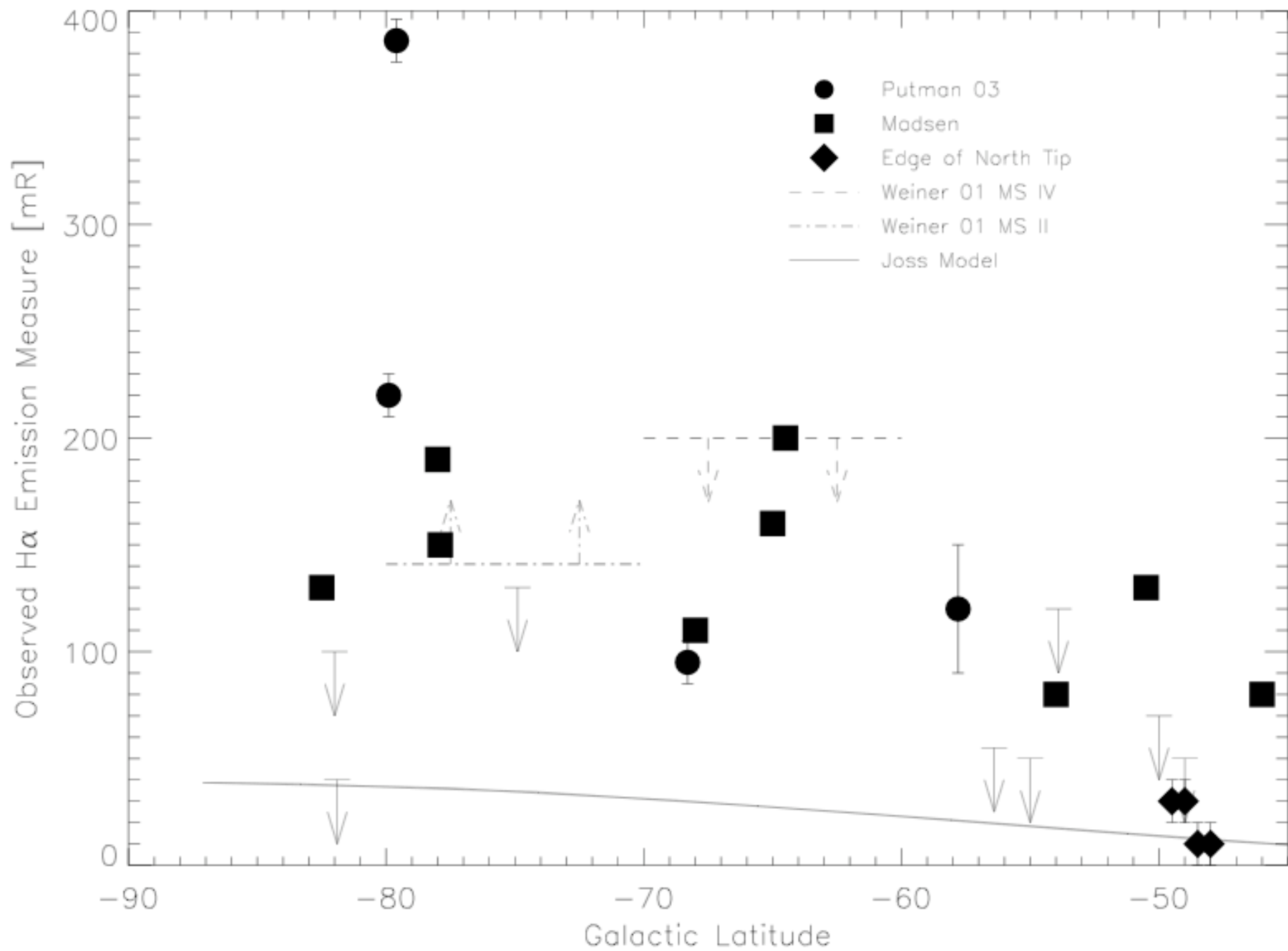
What does this teach us about the Galaxy?

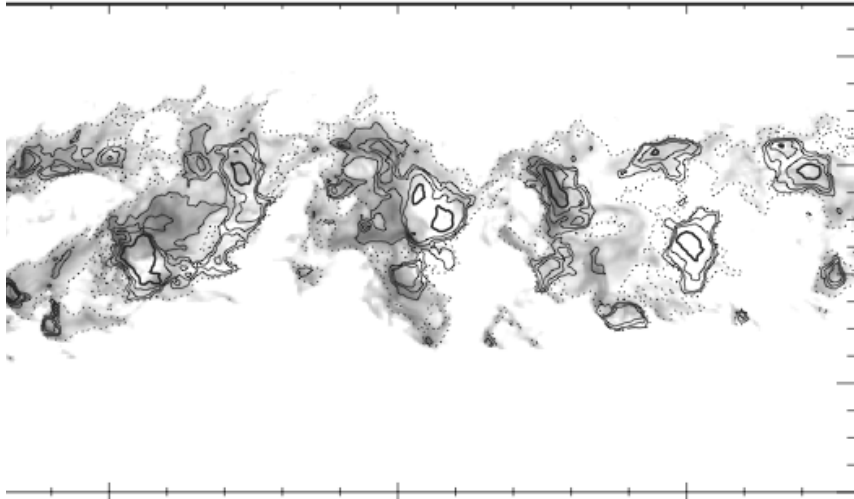
Seyfert NGC 7213 ionizes gas stream at $r \sim 30$ kpc



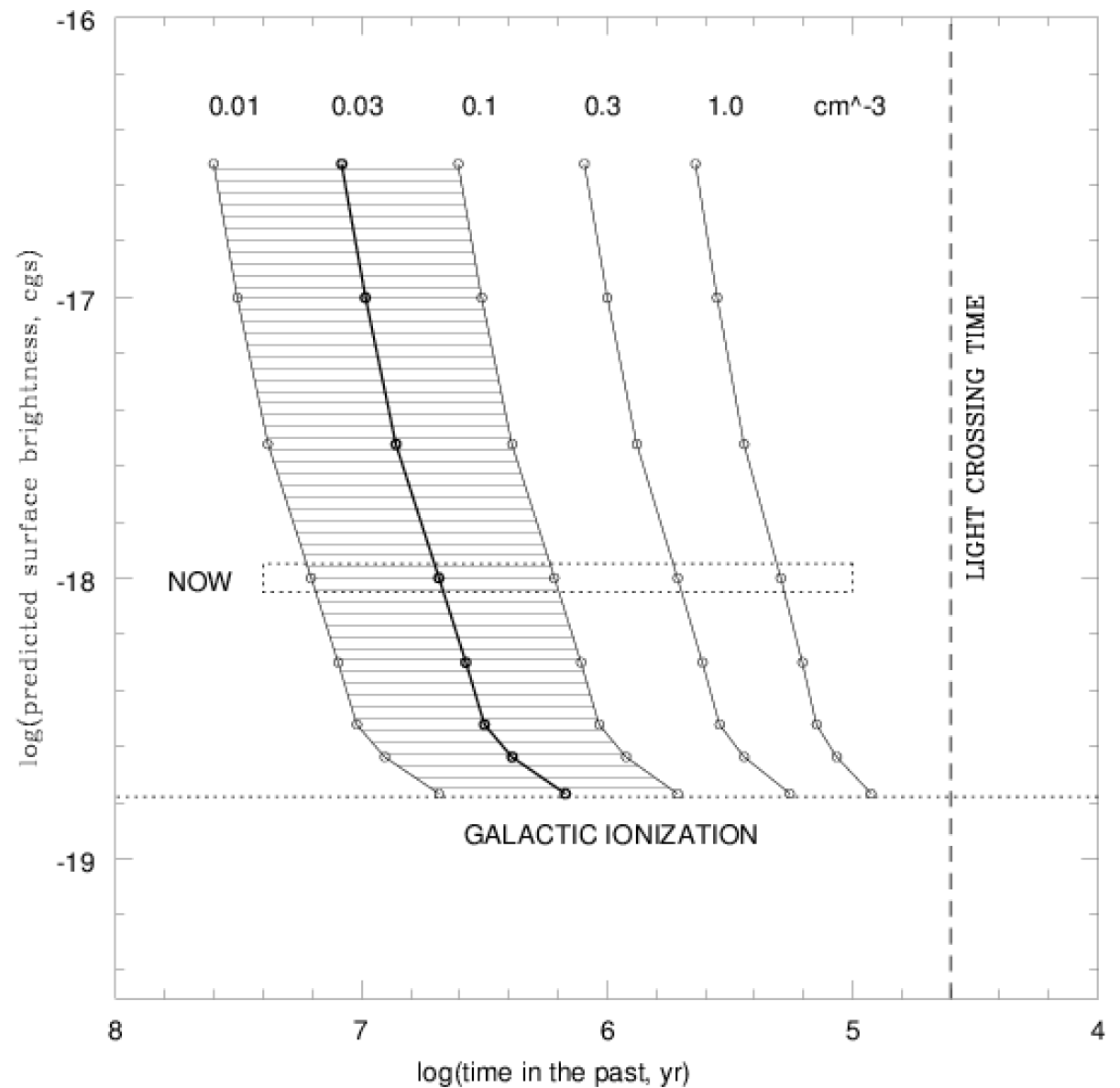
The Magellanic HI Stream







If a past ionizing event (e.g. Seyfert phase) took place at a time T_0 then it would show up in the plasma where $T_{\text{rec}} \sim T_0$.



$$\mu(\text{H}\alpha) = 1.1 \times 10^{-18} b \left(\frac{fE}{0.1} \right) \left(\frac{r}{55 \text{ kpc}} \right)^{-2} \text{ cgs}$$

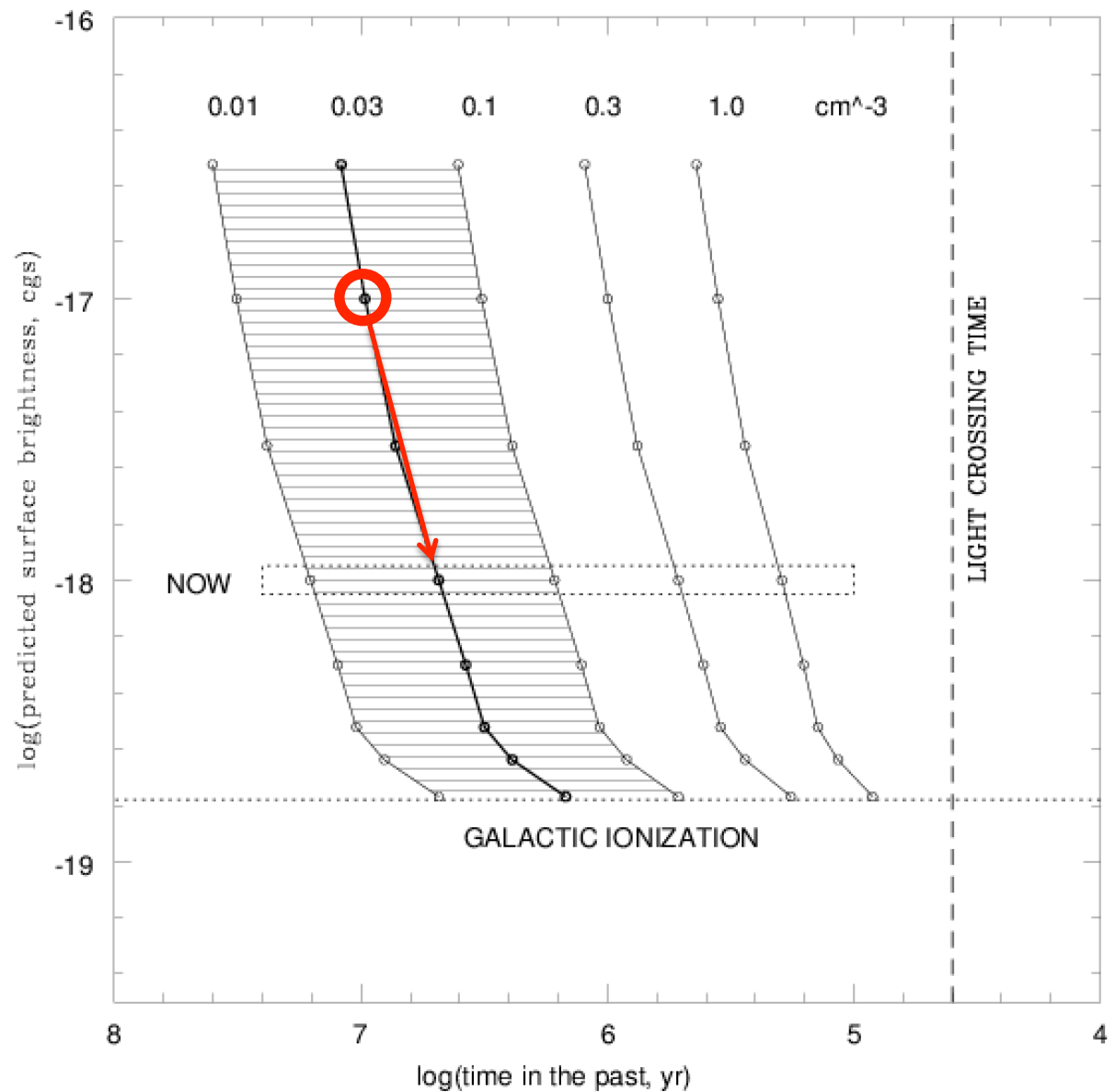
If Proga & Kallman (2004) are right, a line driven wind from the GC black hole must be close to $f_E = 1$.

This generates strong UV and a wind that reaches 1 kpc in 10^5 yr, 10 kpc in 1 Myr.

The Stream density is $\sim 0.03 \text{ cm}^{-3}$ suggesting a Seyfert event ~ 10 Myr ago.

The present jet/bubble would need to arise from a later episode.

New COS data can test this model, and the possible poloidal field.



$$\mu(\text{H}\alpha) = 1.1 \times 10^{-18} b \left(\frac{f_E}{0.1} \right) \left(\frac{r}{55 \text{ kpc}} \right)^{-2} \text{ cgs}$$

The Future:

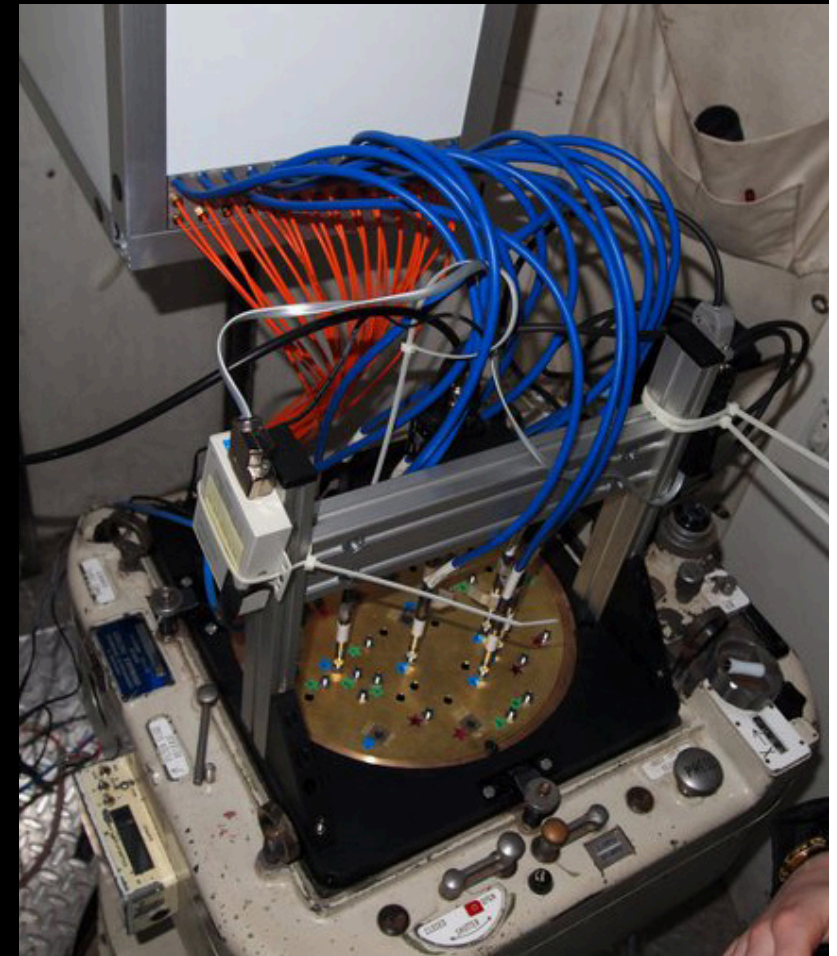
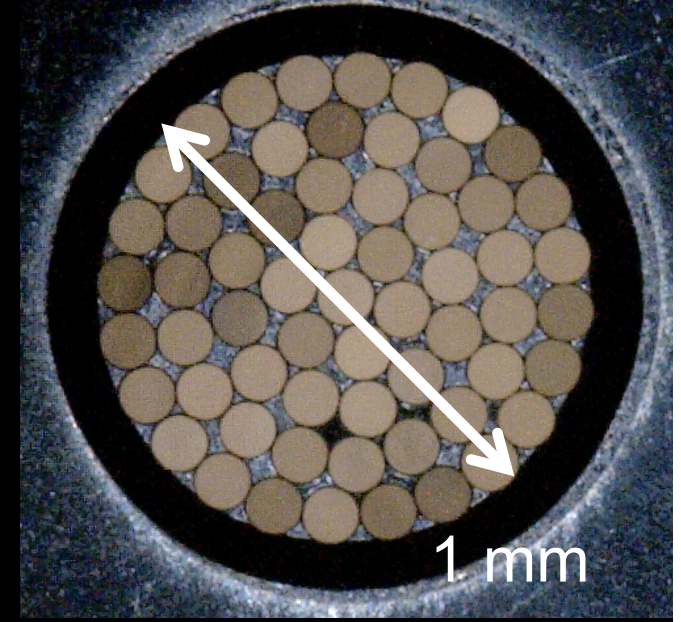
the first major search for galactic winds

Sydney-AAO Multibundle Instrument – **SAMI**

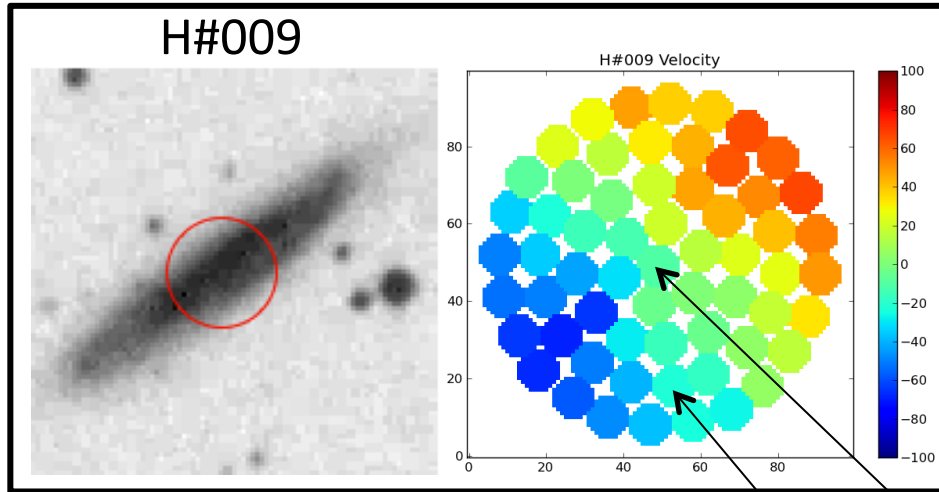
10 months from concept to first light...

$R \sim 5000$ (370-550 nm, 620-740 nm)

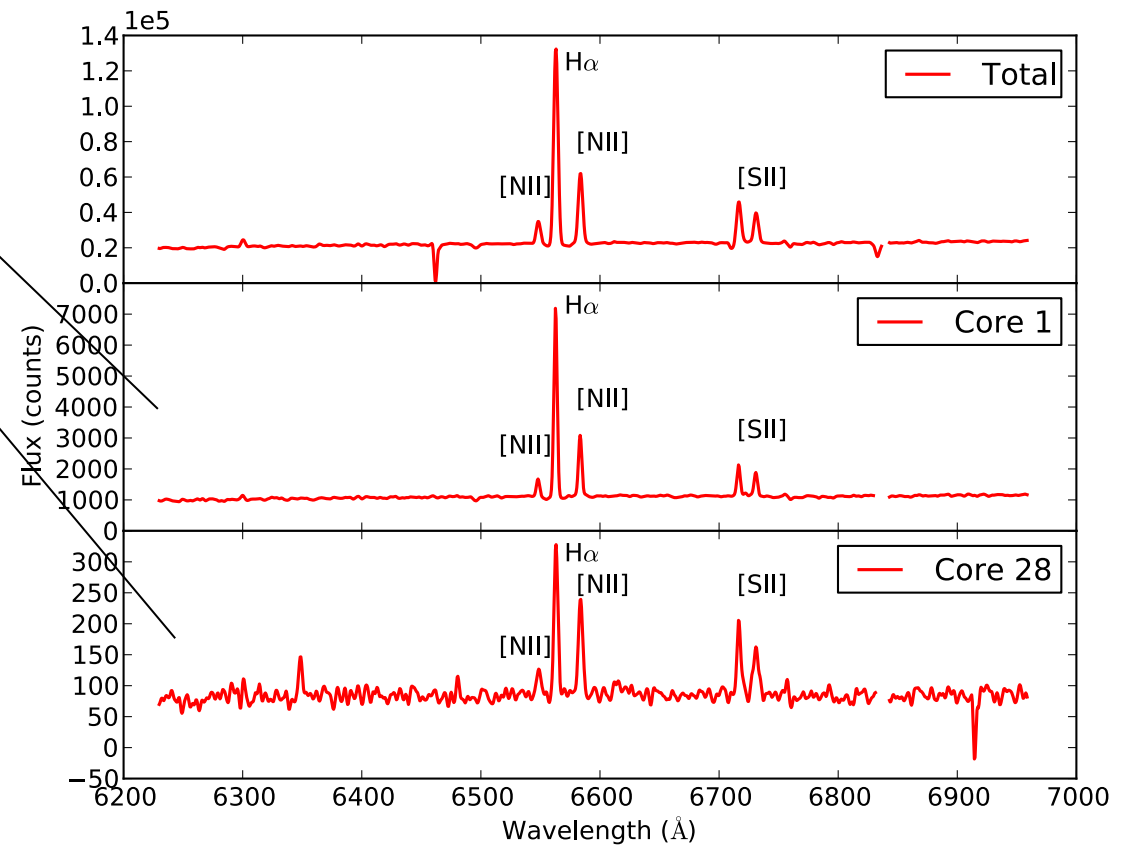
Croom+ 2012, MNRAS



SAMI first data (2011)

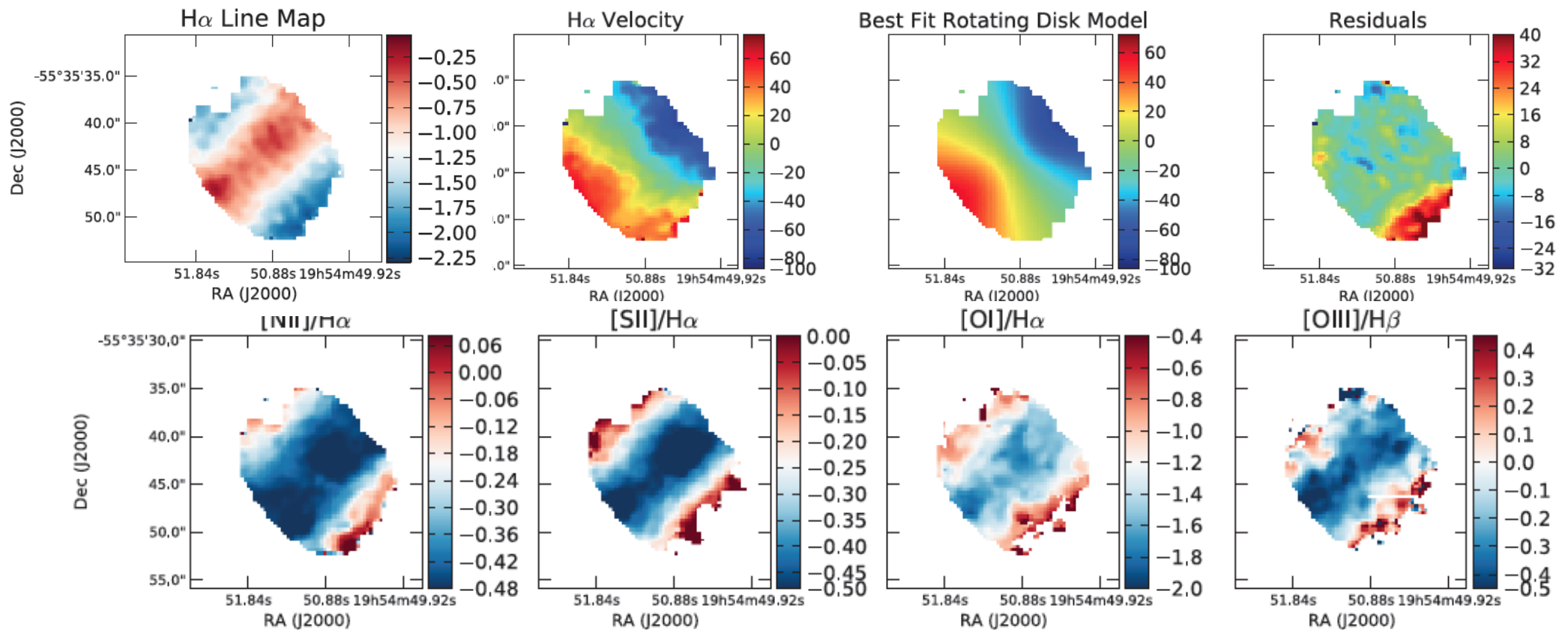
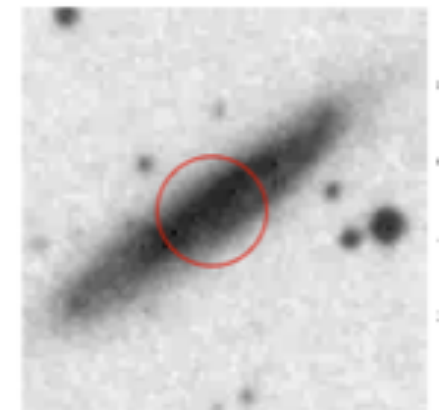


$$b_J = 15.4$$



In the next slide, we show excellent results from dithering over 4 hours

SAMI first science: serendipitous galactic wind



All 13 galaxies are dithered in the same fashion

Fogarty et al. (2012)

Final thoughts

We can clearly separate AGN from ★B driven winds for galaxies with $L = 1-10 \times 10^{10} L_0$.

The imprint of past AGN activity may be visible across the Magellanic Stream. We can look for this with COS absorption line data.

A much larger sample of galactic winds will soon emerge from the SAMI survey.

Question:

For the same input energy, how different are AGN driven winds from ★B driven winds? Are AGN winds always accompanied by strong UV?